

Analysis of Single-Pion Production Reactions $\pi + N \rightarrow \pi_1 + \pi_2 + N'$ below 1 BeV*

M. G. OLSSON†

University of Wisconsin, Madison, Wisconsin

AND

G. B. YODH

University of Maryland, College Park, Maryland

(Received 14 January 1966)

A phenomenological investigation of the low-energy pion production process has been carried out using an amplitude for s -wave N^* production as well as a totally isotropic amplitude. It is found that these two amplitudes in $T=\frac{3}{2}$ and $T=\frac{1}{2}$ isotopic-spin channels will give a reasonable explanation of most of the experimental data below 700 MeV. A detailed comparison with experimental data in five single-pion production reactions is carried out to determine the seven model parameters. The analysis shows (i) that the $T=\frac{3}{2}$ reactions are explained by constant amplitudes and phases in the P_{31} and D_{33} states; (ii) that the D_{13} inelastic phase must rise through 90° near 600 MeV; and (iii) that there must be a significant P_{11} amplitude. The model does not account for the peaking of the $\pi^+\pi^-$ mass at the upper end of the phase space. Possible causes of this $T=0$, $\pi\pi$ enhancement are discussed.

I. INTRODUCTION

A PHENOMENOLOGICAL analysis of the single-pion production reactions $\pi + N \rightarrow \pi_1 + \pi_2 + N'$ below 1 BeV is presented in this paper. We have attempted to construct a model which is realistic enough to be able to fit the experimental data, but yet makes a minimum of assumptions about the underlying dynamics.

The usual "isobar model" of Lindenbaum and Sternheimer¹ has been generalized to include (i) final-state scattering effects from all attractive interactions between pairs of particles; (ii) interference terms which arise because in the final state the nucleon can be shared by both pions; (iii) the angular-momentum properties of the "isobar" in its decay. The well-established attractive pion-nucleon interactions in the low-energy region (π - N mass < 1500 MeV) are (i) the $T=\frac{3}{2}$, $J=\frac{3}{2}$ p -wave pion-nucleon resonance at 1236 MeV, henceforth called $N^*(3,3)^+$ (or $P_{3/2}^+$) and (ii) the $T=\frac{1}{2}$, $J=\frac{1}{2}$ s -wave scattering interaction ($S_{1/2}^-$), described by the α_1 phase shift. These states are assumed to be the dominant final-state attractive interactions contributing to the $\pi_1 + \pi_2 + N'$ state. In this region, below 1 BeV, ρ -meson production can be neglected.

It is shown that in order to account for the experimental data, the following partial waves must dominate in isotopic spin- $\frac{3}{2}$ and $-\frac{1}{2}$ states:

$$D_{3/2}^- \rightarrow (s, P_{3/2}^+)_{3/2}^-$$

and

$$P_{1/2}^+ \rightarrow (s, S_{1/2}^-)_{1/2}^+,$$

where the incoming partial wave is given on the left, and the right-hand side describes the rescattering of

the $N^*(3,3)^+$ and α_1 in s states, respectively. Clearly, there is enough energy to produce the "isobar" in p states and indeed p states may be present as background, but this analysis suggests that s waves dominate. This matter is discussed further in another paper.²

Corresponding to $D_{3/2}^-$ and $P_{1/2}^+$ states in total isotopic spin- $\frac{3}{2}$ and $-\frac{1}{2}$ states, there are seven independent parameters in this analysis: four amplitudes and three phases. By comparison of the prediction of this model with experiment, it is shown that the $T=\frac{3}{2}$ amplitudes and phases are constants, determined by π^+p reactions. However, the $T=\frac{1}{2}$ amplitude and phase describing the $D_{3/2}^-$ partial wave are shown to change rapidly, there being a resonance in the region near $T_\pi = 600$ MeV.

The analysis does not describe the $\pi^+\pi^-n$ system adequately. The data indicate that there may be some $\pi\pi$ interaction³ in the isotopic spin-zero state or some dynamical effect not describable by this model.⁴

The organization of the paper is as follows: In Sec. II we summarize the experimental situation below 1 BeV, pointing out the important features of the data. These are used in developing the model and evaluating the parameters in later sections. In Sec. III we review the previous attempts at analyzing the single-pion production data using dynamical as well as phenomenological theories. The inadequacies of these models are discussed and the present analysis is motivated. In Sec. IV is presented a detailed description of the "Olsson-Yodh" model, stating clearly the parameters involved. In Sec. V the predictions of the model are compared with experimental data and a phenomenological analysis is carried out. Section VI contains a compilation of the experimental references used in the

* Supported in part by the U. S. Atomic Energy Commission.

† Based on a Ph.D. thesis, M. G. Olsson, University of Maryland, June, 1964 (unpublished).

¹ R. M. Sternheimer and S. J. Lindenbaum, Phys. Rev. **110**, 1723 (1958); **105**, 1874 (1957); **106**, 1107 (1957); and **123**, 333 (1961).

² M. Olsson and G. B. Yodh, Bull. Am. Phys. Soc. **10**, 35 (1965); G. B. Yodh and M. Olsson, following paper, Phys. Rev. **145**, 1327 (1966).

³ ρ production is neglected as the threshold for its production is at the upper end of the energy region considered in the paper.

⁴ V. Anisovich and L. Dakhno, Phys. Letters **10**, 221 (1964).

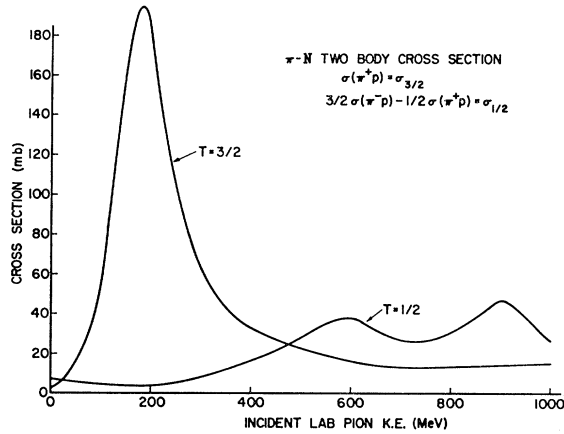
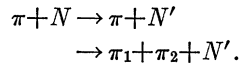


FIG. 1. The two-body isotopic-spin cross sections.

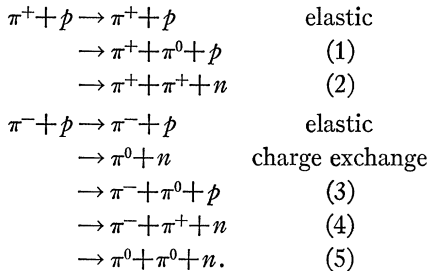
analysis. Finally, in Sec. VII we summarize our conclusions and discuss the inadequacies of the model herein developed.

II. THE EXPERIMENTAL SITUATION BELOW 1 BeV

Let us discuss the reactions



Even if we confine ourselves to the experimentally favorable cases where the target nucleon is a proton and the incident pions are charged (π^+ or π^-), the isotopic-spin structure can be completely investigated. In these cases the reactions to consider are



The cross sections measured in the above reactions may be expressed in terms of pure isotopic-spin cross sections by means of the following well-known relations:

$$\begin{aligned} \sigma_{3/2} &= \sigma(\pi^+ p) \\ \sigma_{1/2} &= \frac{3}{2}\sigma(\pi^- p) - \frac{1}{2}\sigma(\pi^+ p), \end{aligned} \quad (2.1)$$

where $\sigma(\pi^\pm p)$ denotes the sum of all final-charge-state cross sections for a given reaction type.

The two-body isotopic-spin cross sections are illustrated in Fig. 1.⁵ In the $T=\frac{3}{2}$ channel the dominance of

⁵ Below 400 MeV we have used the compilation of N. Klepikov *et al.* [N. Klepikov, V. Meshcheryakov, and S. Sokolov, JINR-D-584, 1960 (unpublished)]. Above 400 MeV the total cross

of the $N^*(3,3)^+$ is evident. Above this resonance the cross section is quite featureless since the fast-rising inelastic component has been removed. The $T=\frac{1}{2}$ cross section at low energy is given by α_1 , the $T=\frac{1}{2}, J=\frac{1}{2}$ s -wave scattering length. Near 600 and 900 MeV there occur peaks which have been designated by spin and parity $\frac{3}{2}^-$ and $\frac{5}{2}^+$, respectively.^{6,7}

Next we consider some of the experimental features of the inelastic reactions. Figure 2 is a rough interpolation of the compiled cross-section data (see Sec. VI).

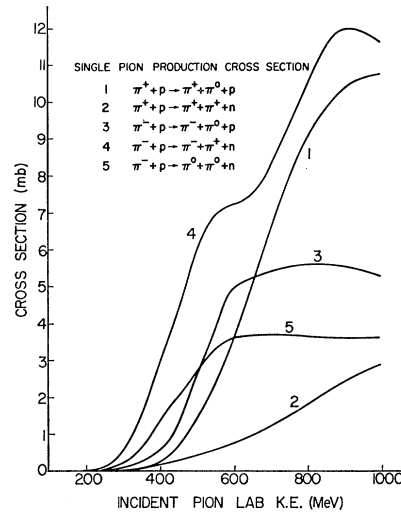


FIG. 2. Inelastic cross sections. For error assignments, see Figs. 8, 9, 20, 21, and 22.

The following points are to be noted:

- (i) Absorption is much stronger for the $T=\frac{1}{2}$ state than the $T=\frac{3}{2}$ states especially at low energies (see Fig. 4 for more detail);
- (ii) $\sigma(\pi^+\pi^0 p)$ rises rapidly;
- (iii) $\sigma(\pi^+\pi^+ n)$ rises relatively slowly;
- (iv) $\sigma(\pi^-\pi^0 p)$ and $\sigma(\pi^0\pi^0 n)$ flatten out above 600 MeV;
- (v) $\sigma(\pi^-\pi^+ n)$ appears to have a shoulder near 600 MeV;
- (vi) $\sigma(\pi^0\pi^0 n)$ rises rapidly in the region $350 < T_\pi < 600$ MeV.

In the analysis to follow the relative growth rates of various inelastic channels provide a powerful tool to determine the important partial waves.

Figure 3 shows the energy variation of the ratio $\sigma(\pi^+\pi^0 p)/\sigma(\pi^+\pi^+ n)$, the ruled area representing the experimental error. The threshold limit (neglecting

sections of T. Devlin *et al.* [T. Devlin, B. Moyer, and V. Perez-Mendez, Phys. Rev. **125**, 690 (1962)] have been used with inelastic cross sections from our compilation (see Sec. VI).

⁶ B. Moyer, Rev. Mod. Phys. **33**, 367 (1961), gives a summary of results.

⁷ P. Baryre, C. Bricman, G. Valladas, and G. Villet, Phys. Letters **8**, 137 (1964); L. Roper, Phys. Rev. Letters **12**, 340 (1964); A. Donnachie, J. Hamilton, and A. T. Lea, Phys. Rev. **135**, B515 (1964); R. F. Peierls, *ibid.* **118**, 325 (1960); P. Auvil and C. Lovelace, Nuovo Cimento **33**, 473 (1964).

small mass-difference corrections) is taken to be $\frac{1}{4}$ because of the Bose symmetry of the final pions.

The relative strength of pion production in $T=\frac{1}{2}$ and $T=\frac{3}{2}$ isotopic-spin states is given in Fig. 4 as a function of T_π . The isotopic-spin cross sections were derived from the experimental compilation by use of Eq. (2.1).

At threshold of pion production all the particles in the final state must be in relative s states. Hence, the dominant transitions are $P_{1/2}^+ \rightarrow (s, S_{1/2}^-)_{1/2}^+$ in $T=\frac{1}{2}$ and $\frac{3}{2}$ states. If the amplitudes for these transitions are called c_1 and c_3 , respectively, then a parameter $R=c_1/c_3$ can be defined which is given by the threshold limit (see Sec. V for details)

$$\sigma(T=\frac{1}{2})/\sigma(T=\frac{3}{2}) \rightarrow \frac{2}{9}R^2. \quad (2.2)$$

In Sec. V we find that $R=-2.8\pm 0.3$. Using this value of R , the threshold value of the ratio (1.2) is 3.2 ± 0.7 .

Figure 5 shows the energy variation of the ratio $\sigma(\pi^-\pi^+n)/\sigma(\pi^-\pi^0p)$ of reactions (3) and (4). Using the magnitude R from above and a result of Sec. V that R

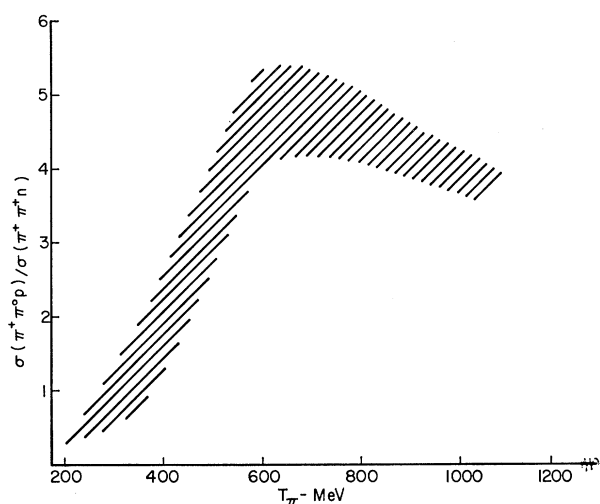


FIG. 3. The ratio $\sigma(\pi^+\pi^0p)/\sigma(\pi^+\pi^+n)$ plotted as a function of incident pion energy. The experimental errors are represented by the ruled region. The threshold limit is given by generalized Bose symmetry.

must be negative (i.e., c_1 and c_3 being 180° out of phase) to fit the angular distributions near threshold, the threshold limit for $\sigma(\pi^-\pi^+n)/\sigma(\pi^-\pi^0p)$ is given by

$$\sigma(\pi^-\pi^+n)/\sigma(\pi^-\pi^0p) \rightarrow (2/9)(2R+1)^2 = 4.7\pm 1.3. \quad (2.3)$$

Note that there seems to be a change in the energy variation of these last two ratios near $T_\pi=400$ MeV which is also the isobar production threshold.

In the three-body final state both the particle energies and the angles are distributed continuously. The most striking feature of the energy distributions is the strong tendency for the pions to come off associated with the nucleon in the $T=\frac{3}{2}$, $J=\frac{3}{2}$ state. This effect is illustrated in Fig. 6 for reaction (1) ($\pi^++p \rightarrow \pi^++\pi^0+p$) at T_π

$=979$ MeV.⁸ The π^+ associates with the proton in a pure $T=\frac{3}{2}$ state and so will be more prominent than the π^0p combination. The curve corresponds to s -wave isobar formation; the shift relative to the experimental curve indicates the importance of higher waves at this energy. The shoulder at $M(\pi^+p)\sim 1400$ is the reflection of π^0p isobar formation.

Finally, it should be pointed out that in the $\pi^-\pi^+n$ system there is consistent peaking near the upper end of the $(\pi^-\pi^+)$ mass spectrum from threshold up to around $T_\pi=700$ MeV.⁹

III. METHODS FOR DEALING WITH LOW-ENERGY SINGLE-PION PRODUCTION

The static model of Chew and Low which had been so successful in low-energy pion-nucleon scattering and photomeson production was applied in 1956 by Rodberg and Kazes¹⁰ to the single-pion production process. The cross sections near threshold that they derived were often over an order of magnitude smaller than experiment.¹¹ In 1958 Lindenbaum and Sternheimer¹ showed that a qualitative understanding of the single-pion-production mass distributions could be gained by assuming that a pion is produced along with a $(3,3)$ isobar which subsequently decays, thus indicating that final-state interactions play an important role.

Enlarging upon previous suggestions that pion-pion scattering effects may be important¹² Rodberg,¹³ using

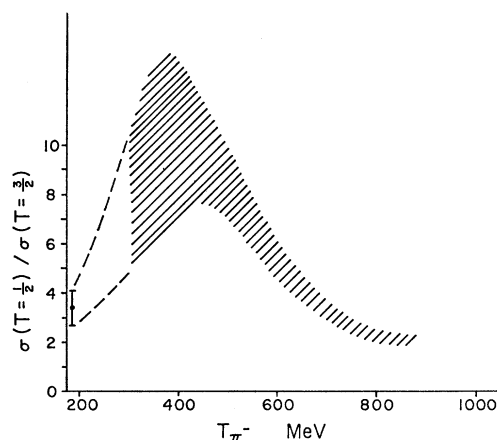


FIG. 4. The experimental ratio of the isotopic spin-absorption cross sections $\sigma(T=\frac{1}{2})/\sigma(T=\frac{3}{2})$. The threshold value is given by (1.2).

⁸ G. Tauffest and R. Willmann, Bull. Am. Phys. Soc. **10**, 114 (1965) and private communication.

⁹ J. Kirz, J. Schwartz, and R. Tripp, Phys. Rev. **130**, 2481 (1963).

¹⁰ L. Rodberg, Phys. Rev. **106**, 1090 (1956); E. Kazes, *ibid.* **107**, 1131 (1957).

¹¹ Results consistent with experiment have however been reported by K. Peng and W. Zoellner, Nucl. Phys. **34**, 491 (1962), and by H. Jahn, Phys. Rev. **126**, 824 (1962).

¹² F. Dyson, Phys. Rev. **99**, 1037 (1955); G. Takeda, *ibid.* **100**, 400 (1955).

¹³ L. Rodberg, Phys. Rev. Letters **3**, 58 (1959).

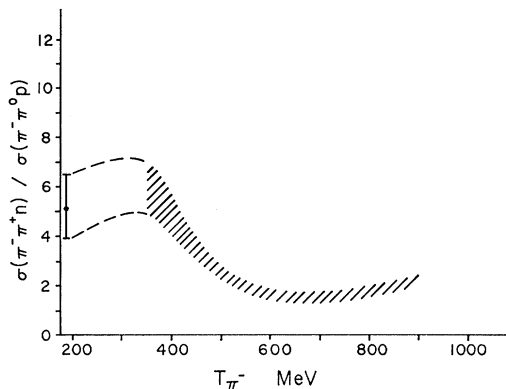


FIG. 5. The energy dependence of the ratio $\sigma(\pi^-\pi^+n)/\sigma(\pi^-\pi^0p)$. The threshold limit is given by (1.3).

a modified static model, was able to show that the single-pion exchange diagram accounts for most production cross sections¹⁴ by assuming quite reasonable s - and p -wave pion-pion scattering lengths but ignoring isobar effects. The success of the isobar model in explaining the energy spectra of the final-state particles led to the suggestion that the single-pion exchange diagram should be modified to allow for the scattering of one of the pions with the nucleon in the (3,3) state.¹⁵ Detailed calculations, allowing for rescattering but still using the static model with pion-pion interactions, were done by Carruthers¹⁶ and by Goebel and Schnitzer.¹⁷ A characteristic of these calculations is that real isobar production cancels. Goebel and Schnitzer have calculated the expected mass distributions of the π^-n combination in the reaction $\pi^-+p \rightarrow \pi^-+\pi^++n$ near isobar production threshold. Their results were in disagreement with the data,⁹ which show a characteristic strong enhancement at large π^-n masses whereas they predict a depression.

A second model which proposes a definite dynamical explanation of pion production is that of ρ exchange.¹⁸ In the energy range below 1 BeV this model fails in two respects. First, the $T=\frac{3}{2}$ amplitude is favored over the $T=\frac{1}{2}$ amplitude in contradiction to the experimental situation (see Fig. 4). Secondly, the N^{*-} isobar cannot be produced in π^-p collisions by ρ exchange whereas it is quite evident in the experimental mass distributions.⁹ It has been conjectured that the dominance of the $T=\frac{1}{2}$ state over the $T=\frac{3}{2}$ state at low energy may be due to a nucleon or a nucleon isobar pole in the s channel.¹⁹

This discussion of production models has been limited to those which were designed to give detailed predictions

¹⁴ W. Perkins, J. Caris, R. Kenney, E. Knapp, and V. Perez-Mendez, *Phys. Rev. Letters* **3**, 56 (1959).

¹⁵ P. Carruthers and H. Bethe, *Phys. Rev. Letters* **4**, 536 (1960); F. Selleri, *Nuovo Cimento* **16**, 775 (1960).

¹⁶ P. Carruthers, *Ann. Phys. (N. Y.)* **14**, 229 (1961).

¹⁷ C. Goebel and H. Schnitzer, *Phys. Rev.* **123**, 1021 (1961); H. Schnitzer, *ibid.* **125**, 1059 (1962).

¹⁸ L. Stodolsky and J. Sakurai, *Phys. Rev. Letters* **11**, 90 (1963); L. Stodolsky, *Phys. Rev.* **134**, B1099 (1964).

¹⁹ F. Selleri, in *Lectures in Theoretical Physics* (University of Colorado Press, Boulder, Colorado, 1964), p. 236.

of the final three-particle states. We have seen that no single dynamical mechanism is capable of explaining single-pion production below 1 BeV; thus it is reasonable to use a more phenomenological approach which ignores production dynamics and concentrates on the partial-wave structure of the amplitude and known rescattering effects. We visualize the production process to proceed by means of the diagram in Fig. 7, where the rescattering vertex can be calculated in terms of elastic pion-nucleon scattering parameters, and the unknown production process is compressed into a single bubble. This is a general form of the usual isobar model. The N^* production vertex can depend on the isobar production angle and momentum, the simplest case being when the isobar is produced isotropically (s -wave production). Figure 7 could have also been drawn with the N^* decaying into π_1 and N . Since the $N^*\pi$ intermediate state is unobserved, we must superpose the amplitudes for each process in the usual quantum-mechanical fashion to calculate the net effect. The error made by neglecting the subsequent interference term is related to the probability that a pion can simultaneously be a "decay" and an "extra" pion. Below 1 BeV a large error is made if one neglects the interference term. If the (3,3) isobar is produced in an s wave, the absorption is from $D_{3/2^-}$. $P_{1/2^+}$, $P_{3/2^+}$, and $F_{5/2^+}$ initial states lead to p -wave isobar production.²⁰ Analysis of two-body pion-nucleon

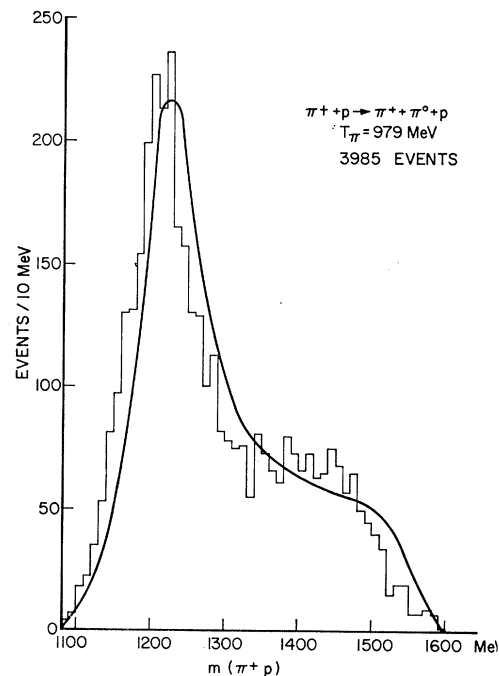


FIG. 6. π^+p mass distribution from the reaction $\pi^++p \rightarrow \pi^++\pi^0+p$ at 979 MeV (Ref. 8) showing a strong tendency for (3,3) isobar formation. The curve is the distribution expected if the isobar is produced in an s wave. The peak shift indicates the importance of p -wave isobar production at this energy.

²⁰ R. F. Peierls, *Phys. Rev.* **111**, 1373 (1958).

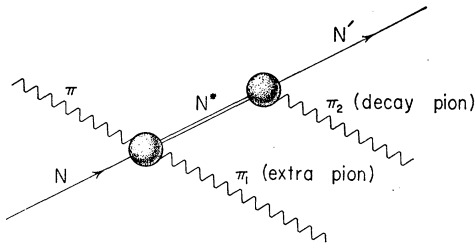


FIG. 7. Isobar model diagram for pion production.

scattering has shown $P_{1/2}$, $D_{3/2}$, and $F_{5/2}$ to be important states in the pion-nucleon system.^{6,7}

The simplest approach, especially at high energies, would be to ignore (i) the complications of angular-momentum states; (ii) assume isotropic isobar production and decay; and (iii) to neglect the interference terms. These assumptions were those of Lindenbaum and Sternheimer's¹ original "isobar model" (henceforth the LS model). In the energy region below 1 BeV, however, it is necessary to coherently add the isobar production amplitudes. Bergia *et al.*,²¹ proposed such a model (in the future referred to as the BBS model) which reduces to the LS model with incoherent addition. They did not, however, stress the need for considering individual partial-wave properties. As we shall see, it is the interference term which is most strongly affected by the choice of partial waves,²² so it is not surprising that the BBS model does not agree at all with experiment since they assume complete isotropy.

Anisovich²³ has suggested a model to be applied at very low energies. He argues that below 450 MeV the interference term becomes smaller and incoherent addition may be a reasonable approximation. This assumption, however, is at best a very crude approximation as the $N^*(1238)$ has a large width. Two relations between the various production cross sections are derived under this assumption. In their corrected form²⁴ they are found to be in poor agreement with experiment, the reason for this being the importance of the totally isotropic [no (3,3) isobar produced] final state at low energies. Anisovich further proposes that the (3,3) isobar be allowed to be produced in both s and p waves. At the low energies considered, he neglects the $F_{5/2}$ absorption and finds that a large variety of angular distributions can be fit with the three incident states. He uses six real parameters to obtain these fits which makes it difficult to determine whether the solution he found is unique.

²¹ S. Bergia, F. Bonsignori, and A. Stanghellini, *Nuovo Cimento* **16**, 1073 (1960).

²² M. Olsson and G. B. Yodh, *Phys. Rev. Letters* **10**, 353 (1963).

²³ V. Anisovich, *Zh. Eksperim. i Teor. Fiz.* **39**, 97 (1960); **39**, 1357 (1960) [English transl.: *Soviet Phys.—JETP* **12**, 71 (1960); **12**, 946 (1961)].

²⁴ The published relations should be corrected by multiplying those cross sections which have identically charged pions by a factor of $\frac{1}{2}$ to avoid counting these pions twice. When this is done, the agreement with experiment is considerably decreased.

Olsson and Yodh²² have considered an isobar model in which the (3,3) isobar is produced in an s wave and decays in a p wave. It was found that by including both the actual angular-momentum properties of the $N^*(3,3)$, as well as the effects of interference between the two production amplitudes,²⁵ the extreme behavior exhibited in the pion energy spectra of the BBS model was rectified. In addition, the model predicts qualitative difference in the pion-pion mass distributions of the various reactions. The experimental data agree quite well with the predictions, a prominent exception being the $\pi^-\pi^+$ mass spectrum from reaction 4. In subsequent reports Olsson and Yodh²⁶ have extended this model to include the well-established two-body attractive interaction $S_{1/2^-}$ (α_1 phase shift) in addition to the $N^*(3,3)$ in the final states. The detailed description of this model and its comparison with experiment is the main subject of this paper.

IV. THE MODEL

A. Preliminaries

Before describing the detailed model, we shall summarize some general results which will provide a framework for our analysis.

A partial-wave transition amplitude may be written as²⁷

$$T^{(J)} = t^{(J)} F(J, f, i),$$

where J (when used as a superscript) denotes the total angular momentum and parity of the state. The $F(J, f, i)$ are 2×2 matrices acting on the nucleon spin and whose elements contain all the angular variables; f and i denote the remaining commuting variables of the final and initial states. The normalization of the angular-momentum projection operators is given by²⁷

$$\text{trace} \int dA F^\dagger(J, f, i) F(J', f', i') = (2J+1) \delta_{JJ'} \delta_{ff'} \delta_{ii'}, \quad (4.1)$$

where dA are the final-particle solid-angle elements in the over-all c.m. system.

Consider the reaction

$$\pi + N \rightarrow \pi_1 + \pi_2 + N'$$

in the over-all center-of-mass system. Let \mathbf{p}_1 , \mathbf{p}_2 , and \mathbf{p}_3 be the momenta of π_1 , π_2 , and N' , respectively. If the

²⁵ R. Dalitz and D. Miller, *Phys. Rev. Letters* **6**, 562 (1961). These authors have used similar amplitudes in their investigation of the effects of Bose symmetry in the reaction $K^- + p \rightarrow \Lambda + \pi^- + \pi^+$.

²⁶ M. Olsson and G. B. Yodh, *Bull. Am. Phys. Soc.* **9**, 27 (1964); University of Maryland Technical Report No. 358, 1964 (unpublished).

²⁷ These projection operators are discussed by V. Ritus, *Zh. Eksperim. i Teor. Fiz.* **32**, 1536 (1957) [English transl.: *Soviet Phys.—JETP* **5**, 1249 (1957)] for the two-body case, and by S. Ciulli and J. Fischer, *Nuovo Cimento* **22**, 264 (1959) for the three-body case. A more general discussion is given by A. Macfarlane, *Rev. Mod. Phys.* **34**, 41 (1962).

target is unpolarized and no polarization is measured, we have

$$|M|^2 = \frac{1}{2} \text{trace} |T_{fi}|^2, \quad (4.2)$$

where

$$T_{fi} = (f|T|i),$$

giving the Dalitz plot density

$$\begin{aligned} \rho(T_1, T_2) &= ((2\pi)^4/qE_0)I, \\ I &= \int d\Omega_1 d\Omega_2 |M|^2 \delta(\mu_{12} - \mu_0), \end{aligned} \quad (4.3)$$

where q is the incident c.m. momentum, μ_{12} is the cosine of the angle between final pion directions in the c.m. system, and

$$\mu_0 = (p_3^2 - p_1^2 - p_2^2)/2p_1p_2.$$

By first rotating the scattering plane about \mathbf{p}_1 , the angular integrations may conveniently be written as

$$\begin{aligned} I &= \int_{-1}^{+1} J(\mu_1) d\mu_1, \\ J(\mu_1) &= 4\pi \int_0^\pi |M|^2 d\lambda_1. \end{aligned} \quad (4.4)$$

The angle λ_1 is given by

$$\mu_2 = \mu_0 \mu_1 + \sin\theta_0 \sin\theta_1 \cos\lambda_1,$$

where μ_1 is the cosine of the polar angle that π_1 makes with the initial direction in the c.m. system. When $J(\mu_1)$ is integrated over T_1 and T_2 , the angular distribution of particle one results. In a similar way the angular distributions of the other particles can be calculated.

An alternative form may also be derived (see Appendix A)

$$J(\mu_1) = 2r^2 \sum_{l=0}^{\infty} (2l+1) \int_{-1}^{+1} d\mu_2 |M|^2 \times P_l(\mu_0) P_l(\mu_1) P_l(\mu_2) \quad (4.5)$$

which is analogous to a result, attributed to Goldberger,²⁸ which arises in the study of the two-particle unitarity integral.

If we parametrize the elastic amplitude in the usual way

$$t_e^{(J)\alpha}(\eta_J e^{i\delta_J} - 1)$$

we can use unitarity of the S matrix to provide bounds on each partial-wave contribution to the inelastic cross section (e.g., Olsson²⁹; Blatt and Weisskopf³⁰):

$$\sigma_{\text{in}}^{(J)} = (\pi/K^2)(J + \frac{1}{2})(1 - \eta_J^2), \quad (4.6)$$

²⁸ R. Omnes, *Nuovo Cimento* **25**, 806 (1962). R. Karplus, University of Maryland Technical Report No. 303, 1963 (unpublished).

²⁹ M. Olsson, Ph.D. thesis, 1964, University of Maryland Technical Report No. 379 (unpublished).

³⁰ J. Blatt and V. Weisskopf, *Theoretical Nuclear Physics* (John Wiley & Sons, Inc., New York, 1952).

where K is the incident wave number in the c.m. system and $0 \leq \eta_J \leq 1$.

In addition, the phase of the production amplitude near inelastic threshold is given by^{29,31}

$$t^{(J)} \xrightarrow{\text{threshold}} \lambda^{(J)} |t^{(J)}|^2 e^{i\delta_J}, \quad (4.7)$$

where $\lambda^{(J)} = \pm 1$ and δ_J is the elastic-scattering phase shift in the same partial wave at inelastic threshold. This result is completely analogous to the "Watson theorem" in two-body reactions.³²

Finally the following observations can be made on the sensitivity of various distributions to the partial-wave structure of the matrix element.

(1) Because the angular integration eliminates the interference between partial waves of differing angular momentum and parity, the Dalitz plot is not sensitive to small admixtures of different partial waves.

(2) The angular distributions are sensitive to interferences between partial waves.

B. The Formulation of the Model

When there are three particles in the final state, it becomes difficult to carry out a phase-shift-type analysis. Not only are there three more variables because of the extra particle, but there is also the additional difficulty of the ambiguity in coupling angular momentum or isotopic spin.

Both the angular momentum and the isotopic spin may be described in either of two ways. In the first, one pion can be coupled to the nucleon and this combination coupled to the second pion (the πN representation). Alternatively, the two pions might be first coupled together and then this combination coupled to the nucleon (the $\pi\pi$ representation). Although both representations are equivalent in a mathematical sense, it may well be that in one representation the amplitude for pion production is approximated by a few terms, while in the other by many.²⁷

In view of the difficulty of a completely general phase-shift analysis, it seems reasonable to use a production amplitude which is still quite general but is of such a form that the most important experimental features of the pion-production process are accounted for. In Fig. 6 we saw that a dominant feature is the production of the $N^*(3,3)$ resonance. This is the physical basis of the conventional isobar model as discussed in Sec. III. We may slightly generalize this idea by postulating that the most important production amplitudes are those in which a pair of particles interact in the final state.

The phenomenon of final-state scattering has been studied by Watson³³ in a potential-scattering model.

³¹ J. Sucher (private communication).

³² K. Watson, *Phys. Rev.* **85**, 852 (1952); R. Dalitz and S. Tuan, *Ann. Phys. (N. Y.)* **3**, 307 (1960).

³³ K. Watson, *Phys. Rev.* **88**, 1163 (1952).

TABLE I. Charge-dependent factors in the pion-production isotropic-spin expansion when there are two mesons of the same charge in the final state. These coefficients are divided by $\sqrt{2}$ to avoid counting particles twice.

Reaction	$a_{3,3}(1)$	$a_{3,3}(2)$	$a_{1,3}(1)$	$a_{1,3}(2)$	$a_{2,1}(1)$	$a_{3,1}(2)$	$a_{1,1}(1)$	$a_{1,1}(2)$
$\pi^+p \rightarrow \pi^+\pi^0p$	$3/\sqrt{15}$	$-2/\sqrt{15}$	0	0	0	$-1/\sqrt{3}$	0	0
$\pi^+p \rightarrow \pi^+\pi^+n$	$-1/\sqrt{15}$	$-1/\sqrt{15}$	0	0	$1/\sqrt{3}$	$1/\sqrt{3}$	0	0
$\pi^-p \rightarrow \pi^-\pi^0p$	$-1/3\sqrt{15}$	$4/3\sqrt{15}$	$\frac{1}{3}\sqrt{\frac{2}{3}}$	$-1/3\sqrt{\frac{2}{3}}$	$-2/3\sqrt{3}$	$-1/3\sqrt{3}$	$2/3\sqrt{3}$	$-2/3\sqrt{3}$
$\pi^-p \rightarrow \pi^-\pi^+n$	$-\sqrt{2/15}$	$\frac{2}{3}\sqrt{2/15}$	$-1/\sqrt{3}$	$-1/3\sqrt{3}$	0	$\frac{1}{3}\sqrt{\frac{2}{3}}$	0	$\frac{2}{3}\sqrt{\frac{2}{3}}$
$\pi^-p \rightarrow \pi^0\pi^0n$	$-\frac{1}{3}\sqrt{1/15}$	$-\frac{1}{3}\sqrt{1/15}$	$\frac{1}{3}\sqrt{\frac{2}{3}}$	$\frac{1}{3}\sqrt{\frac{2}{3}}$	$1/3\sqrt{3}$	$1/3\sqrt{3}$	$-1/3\sqrt{3}$	$-1/3\sqrt{3}$

He finds that transition rates and mass spectra are enhanced only by attractive final-state scattering. In our energy region the only attractive pion-nucleon phase shifts are the ($T=\frac{3}{2}, J=\frac{3}{2}$) resonant amplitude and the ($T=\frac{1}{2}, J=\frac{1}{2}$) α_1 phase shift. The rescattering part of the pion-production amplitude is given entirely in terms of known pion-nucleon scattering parameters. The remaining part can be thought of as a "reduced amplitude." The process can now be defined in terms of the angular momentum of the particle not participating in the final-state scattering. As was discussed in the last section for $N^*(3,3)^+$ rescattering this leads to a set of partial-wave production amplitudes characterized by total angular momentum and parity. For α_1 rescattering, absorption occurs in $P_{1/2}^+$ state if the "extra" pion is isotropic and $S_{1/2}^-$ or $D_{3/2}^-$ if it is a p wave. As mentioned before, we neglect $\pi\pi$ rescattering effects.

The production amplitude may also be expanded into amplitudes of definite isotopic spin. Following the notation of Carruthers³⁴ (μ is the isotopic spin of the intermediate pion-nucleon configuration in the πN representation and T is the total isotopic spin), we see that the production amplitude may be expressed as a sum of four terms.

$$T(\mathbf{p}_1\alpha, \mathbf{p}_2\beta) = \sum_{T\mu} a_{2T,2\mu}(\alpha, \beta) T_{2T,2\mu}(\mathbf{p}_1, \mathbf{p}_2), \quad (4.8)$$

where α is charge state and \mathbf{p}_1 the momentum of pion one. The coefficient $a_{2T,2\mu}(\alpha, \beta)$ term contains all the charge dependence and is a product of Clebsch-Gordan coefficients.

If this amplitude is to exhibit Bose symmetry, we must add a similar term in which the labels of pions one and two are exchanged; that is, the production amplitude must obey the equation

$$T(\mathbf{p}_1\alpha, \mathbf{p}_2\beta) = T(\mathbf{p}_2\beta, \mathbf{p}_1\alpha).$$

In the πN representation this corresponds to allowing either pion to rescatter with the nucleon. Using the notation $a_{2T,2\mu}(1)$ to denote that pion one is rescattering, we can calculate the charge-dependent coefficients for all the single-pion production reactions, as is shown in Table I. Pion one is a π^+ in π^+p reactions and a π^- in π^-p reactions.

The amplitude T [Eq. (4.8)] can be decomposed, first into partial-wave amplitudes t^J ; then t^J can be

separated into a "reduced" matrix element Z for production of the "isobar" times a rescattering part.

The unknown "reduced" matrix element for "isobar" production is characterized by a complex zero-energy scattering length

$$Z = (q/\mu_i)^{l_i} (P/\mu_f)^{l_f} Z_0 e^{i\phi}, \quad (4.9)$$

where q is the incident c.m. momentum, μ_i is the reduced mass of the incident particles whose orbital angular momentum is l_i . The "extra" pion has momentum P and angular momentum l_f ; μ_f is the reduced mass of this pion and the remaining particles.

In the case of $N^*(3,3)^+$ rescattering we may consider the "reduced" matrix element to be the amplitude for the process $\pi + N \rightarrow \pi + N^*$. From the requirement that the cross section for this process cannot depend upon decay parameters of the N^* in the sharp isobar limit^{21,29} the energy-dependent part of the N^* decay amplitude is

$$R = (\Gamma/2\pi p')^{1/2} (\omega_0 - \omega - \frac{1}{2}i\Gamma)^{-1},$$

where p' is the momentum in the N^* rest frame, and the parameters ω_0 and Γ are given in Ref. 35. The model production amplitude [in the case of $N^*(3,3)^+$ production] now becomes

$$T_{2T,3}(J) = -(E_0/\pi) Z R F(J, f, i), \quad (4.10)$$

where Z is given in (4.9) and $F(J, f, i)$ is the angular projection operator which has been calculated previously and explicit expressions may be found in Refs. 27 and 36.

In the case of nonresonant final α_1 state scattering, we take the production amplitude to be

$$T_{2T,1}(J) = -(E_0/m\pi) Z E F(J, f, i), \quad (4.11)$$

$$E = (1 - ik a_s)^{-1},$$

where m is the pion mass, a_s is the $T=\frac{1}{2}, J=\frac{1}{2}$ S -wave π - N scattering length,³⁷ k is the rescattering πN rest-frame wave number, and E is an "enhancement factor."³⁸

³⁵ J. Orear, Nuovo Cimento 4, 856 (1956); N. Klepikov, V. Meshcheryakov, and S. Sokolov, Dubna Report D-584, 1960 (unpublished); M. Olsson, Phys. Rev. Letters 14, 118 (1965); M. Gell-Mann and K. Watson, Ann. Rev. Nucl. Sci. 4, 219 (1954).

³⁶ A FORTRAN program to calculate the experimental consequences of various amplitudes is described by G. B. Yodh, University of Maryland Technical Reports Nos. 442 and 512, 1965 (unpublished).

³⁷ J. Orear, Nuovo Cimento 4, 856 (1956); J. Hamilton, T. Spearman, and W. Woolcock, Ann. Phys. 17, 1 (1962).

³⁸ Enhancement factors have been discussed recently by M. Jacob, G. Mahoux, and R. Omnes, Nuovo Cimento 23, 838 (1962); J. Jackson and G. Kane, *ibid.* 23, 444 (1962).

³⁴ P. Carruthers, Ann. Phys. (N. Y.) 14, 229 (1961).

By comparing the form of Z [as defined in (4.9)] with the form required by unitarity (4.7), we see that near-pion-production threshold Φ must approach the two-body phase shift δ_J (at this energy). In practice this means that Φ is constrained to become small (say $< 15^\circ$) at threshold⁷ (except when absorption is from an incident $T=\frac{3}{2}, J=\frac{3}{2}$ state). The sign of the amplitude at threshold is given by the sign of Z_0 . Since the angular-momentum-barrier terms have been inserted, the production-scattering length Z_0 has the virtue that near threshold it is not only real but also energy-independent.

Of course, our model amplitudes are not inherently unitary for large energies, and hence, the cross sections will eventually exceed the maximum allowed by the inelastic unitarity relation given in (4.6). This situation can be rectified in a nonrigorous way by keeping the production parameter fixed until the unitarity limit is approached and by then decreasing Z_0 such that $\eta_J=0$.

The rescattering amplitude is to be calculated in the rest system of the interacting pion and nucleon. To transform angles back to the over-all c.m. the following transformations are useful (as derived in Appendix B)

$$\begin{aligned} \mathbf{p}'_1 &= \mathbf{p}_1 + X_1 \mathbf{p}_2; & \mathbf{p}'_2 &= \mathbf{p}_2 + X_2 \mathbf{p}_1; \\ X_1 &= (E_1 + E_1') / (E_0 - E_2 + \omega_{13}); & (4.12) \\ X_2 &= (E_2 + E_2') / (E_0 - E_1 + \omega_{23}), \end{aligned}$$

where E_1' is the total energy of pion one in the rest frame of pion one and the nucleon, and ω_{13} is the total energy of this pair.

In the nonrelativistic limit (which is relevant since nonrelativistic angular-momentum concepts have been used)

$$X_1 \approx X_2 \approx m / (M + m),$$

where m is a pion mass and M is the nucleon mass.

In this paper we will only consider the case of isotropic "extra" pion production. This corresponds to $D_{3/2}^-$ and $P_{1/2}^+$ absorption from the initial state for $N^*(3,3)$ and α_1 rescattering, respectively. Higher wave isobar production is certainly possible, in general, and will be dealt with in a later paper.² However, it is found that the great majority of single-pion-production phenomena may be understood by use of only these two partial waves.

We shall now discuss in more detail the process of s -wave $N^*(3,3)$ isobar production. The same isobar may be produced by absorption from either $T=\frac{1}{2}$ or $\frac{3}{2}$ initial states; therefore, we define the relations (using Table I)

$$\begin{aligned} a &= a_{3,3}(1)a_3 + a_{1,3}(1)a_1 e^{i\Phi}, \\ b &= a_{3,3}(2)a_3 + a_{1,3}(2)a_1 e^{i\Phi}, \end{aligned} \quad (4.13)$$

where a_1 is the production parameter Z_0 in the case of $T=\frac{1}{2}$ absorption and a_3 is the production parameter in the case of $T=\frac{3}{2}$ absorption. Since the $T=\frac{3}{2}$ production phase Φ_3 is expected to be smaller than the $T=\frac{1}{2}$ phase

Φ_1 , and since there is one unobserved phase (because the total amplitude has to be squared), we refer all phases to Φ_3 . Thus in this case we define

$$\Phi = \Phi_1 - \Phi_3.$$

Also we shall by convention take a_3 to be positive.

Using this notation the production amplitude (4.10) in the $D_{3/2}$ case becomes

$$T_0 = -(E_0 q^2 / \mu_i^2 \pi) [aR(1)F(1) + bR(2)F(2)], \quad (4.14)$$

where

$$\begin{aligned} R(1) &= (\Gamma_1 / 2\pi p_1')^{1/2} (\omega_0 - \omega_{13} - \frac{1}{2} i \Gamma_1)^{-1}, \\ F(1) &= (4\pi)^{-3/2} (\boldsymbol{\sigma} \cdot \hat{p}_1' - 3\hat{q} \cdot \hat{p}_1' \boldsymbol{\sigma} \cdot \hat{q}), \end{aligned}$$

where \hat{p}_1' and \hat{q} are the directions of p_1' and q .

Using the integration procedure (4.4) we integrate over angles and find the Dalitz plot density

$$\begin{aligned} \rho_D(T_1, T_2) &= (40\pi E_0 q^3 / \mu_i^4) (|aR(1)|^2 + |bR(2)|^2 \\ &\quad + 2\mu_0' \operatorname{Re}[aR(1)b^*R^*(2)]), \end{aligned} \quad (4.15)$$

where $\mu_0' = \hat{p}_1' \cdot \hat{p}_2'$. $\rho(T_1, T_2)$ is measured in mb MeV⁻² if a and b are in fermis.

Note that if we neglect the effect of the angle transformation to the isobar c.m. system, μ_0' is just the cosine of the angle between the pions in the over-all c.m. system.

In a similar way, for $P_{1/2}$ absorption with α_1 rescattering we may define

$$\begin{aligned} c &= e^{i\chi} (a_{3,1}(1)c_3 + a_{1,1}(1)c_1 e^{i\theta}), \\ d &= e^{i\chi} (a_{3,1}(2)c_3 + a_{1,1}(2)c_1 e^{i\theta}), \end{aligned} \quad (4.16)$$

where

$$\theta = \theta_1 - \theta_3, \quad \text{and} \quad \chi = \theta_3 - \Phi_3.$$

Thus for the $P_{1/2}$ case we may write down the total amplitude from (4.11).

$$T_p = (E_0 q / m \mu_i \pi) [cE(1) + dE(2)] \boldsymbol{\sigma} \cdot \hat{q} / (4\pi)^{3/2} \quad (4.17)$$

as in the $D_{3/2}$ case we may integrate over angles and find the Dalitz plot density

$$\rho_p(T_1, T_2) = (10\pi E_0 q / m^2 \mu_i^2) |cE(1) + dE(2)|^2. \quad (4.18)$$

In summary, this model has seven independent (energy-dependent) parameters:

$$\begin{aligned} T=\frac{3}{2} \quad D_{3/2}: & a_3, \\ T=\frac{3}{2} \quad P_{1/2}: & c_3, \chi, \\ T=\frac{1}{2} \quad D_{3/2}: & a_1, \Phi, \\ T=\frac{1}{2} \quad P_{1/2}: & c_1, \theta. \end{aligned}$$

The production parameters Z_0 should be constant only if the "effective range" of the primary interaction is small. Upon comparing the model amplitudes with experiment it is found that the $D_{3/2}$ parameter a_3 is indeed quite constant implying that Watson's criteria³³ for final-state interaction are satisfied. In the $P_{1/2}$ case it is found that the production parameter c_3 must de-

crease somewhat with increasing energy. This dependence can be accounted for with a form factor of the following type

$$F(q) = m^2 / (q^2 + m^2). \quad (4.19)$$

V. COMPARISON WITH EXPERIMENT

The predictions made with various model amplitudes may be compared with experimental data with the following independent quantities:

- a. energy distributions of the three particles or, equivalently, the mass distributions of the three pairs of particles;
- b. angular distributions of the three particles in the over-all center-of-mass system;
- c. the dependence of the reaction cross section on the total energy in the center-of-mass system.

These experimental features for the five production reactions studied comprise an enormous amount of data to be explained. Before describing in detail this comparison, we summarize the main conclusions reached in this section:

1. Final-state interaction seems to dominate almost all aspects of the data; however, by use of the model we are able in some cases to draw conclusions about the "primary process."
2. It is strongly indicated that below $T_\pi = 700$ MeV the $P_{1/2}$ and $D_{3/2}$ absorption amplitudes dominate in both isotopic-spin states.
3. The energy dependence of the cross sections near threshold is accounted for by constant production parameters.
4. The single-pion-production data provide evidence that the $T = \frac{1}{2} N^*(1512)$ resonance in the two-body channel is in the spin and parity state $\frac{3}{2}^-$.
5. An anomalous effect occurs in the $T=0$ $\pi\pi$ mass spectra.

In order to see how the properties of this model differ from those of other isobar models (i.e., LS or BBS models), we shall consider further the expression (4.14) for the Dalitz plot density. Along the line bisecting the Dalitz plot ($T_1 = T_2$), the density is proportional to

$$\rho \propto \{ |a|^2 + |b|^2 + 2\mu_0' \operatorname{Re}(a^*b) \}. \quad (5.1)$$

Here increasing pion kinetic energy corresponds to increasing π - π mass, and μ_0' varies from +1 at the minimum π - π mass to -1 at the maximum π - π mass. The quantities a and b measure the probability for production of the two isobar charge states. Thus, the π - π mass distribution is sensitive to the last term, which arises from interference between the two isobar production processes. In the LS model the interference term is absent so that the π - π mass distribution will resemble phase space for all reactions. The BBS model would correspond to the absence of the term μ_0' in (5.1) because it arises from the p -wave nature of

$N^*(3,3)$ decay. Therefore, in the BBS model the π - π mass distributions will resemble phase space. However, in this model for reactions in which $a \approx -b$ there is the possibility of depletion along the Dalitz plot bisector.²² In our model the presence of the μ_0' term introduces a peaking in the high or low end of the π - π mass distribution depending on whether the sign of the real part of a^*b is negative or positive. In the case of p -wave isobar production the interference term will no longer be linear in μ_0' .

Next we examine the $T = \frac{3}{2} \pi^+ p$ system where only two amplitudes are considered.

A. $\pi^+ p$ Reactions

There are two reactions to be considered in this case:

- (1) $\pi^+ + p \rightarrow \pi^+ + \pi^0 + p$
- (2) $ \rightarrow \pi^+ + \pi^+ + n.$

The parameters which enter are a_3 , c_3 , and χ . Only the magnitudes of the real numbers a_3 and c_3 are needed to determine the cross sections and energy distributions. The angular distributions are sensitive to the sign of c_3 (a_3 is positive by convention) and to χ . In addition, by unitarity, χ becomes small at low energies.

Above isobar production threshold (about $T_\pi = 400$ MeV) we expect that s -wave isobar production will be dominant over some finite interval until p and higher waves come in. If s -wave production ($D_{3/2}$) were the sole mechanism, the ratio of cross sections for reaction (1) to reaction (2) would be 5.5. By referring to Fig. 3, it is seen that this ratio rises to a maximum of roughly 4.5 at $T_\pi = 600$ MeV. At higher energies this ratio gradually falls, perhaps due to the onset of higher partial-wave isobar production. Thus near 600 MeV the $D_{3/2}$ state could be the dominant partial wave.

If $P_{1/2}$ absorption (with α_1 rescattering) were the only contributing process, the cross-section ratio of reaction (1) to reaction (2) would be $\frac{1}{4}$. This amplitude is completely isotropic in the final state and thus will become dominant as threshold is approached. As a result, the rapid fall of the cross-section ratio (Fig. 3) at low energies is accounted for if $P_{1/2}$ absorption is the dominant mechanism near threshold.

At a given T_π the cross sections for reactions (1) and (2) enable one to determine the magnitudes of a_3 and c_3 . Since experimental data is available over the energy range in question, we are able to determine $|a_3|$ and $|c_3|$ as a function of energy. It is found that an adequate fit to both excitation functions is obtained with constant-production parameters,³⁶

$$\begin{aligned} |a_3| &= 0.0175 \pm 0.0008 \text{ F}, \\ |c_3| &= 0.102 \pm 0.006 \text{ F}. \end{aligned} \quad (5.2)$$

The comparisons of the model predictions using these values are shown in Fig. 8 for reaction (1) and in Fig. 9 for reaction (2). In these figures the lower solid line is

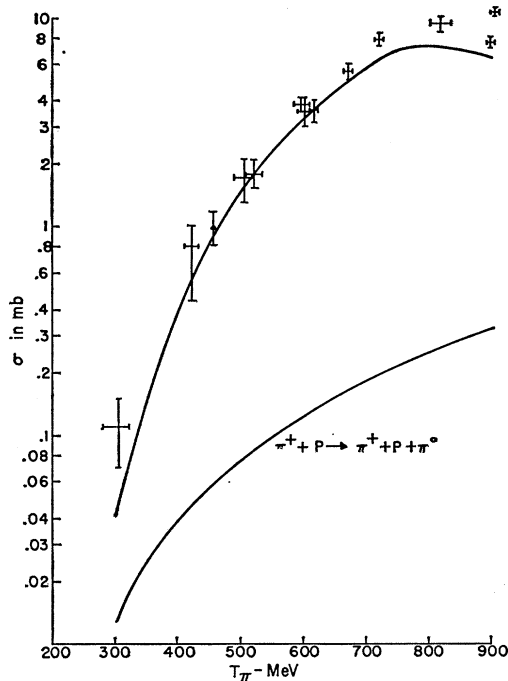


FIG. 8. Cross sections for the reaction $\pi^+ + p \rightarrow \pi^+ + \pi^0 + p$. The upper curve is calculated using both the $P_{1/2}$ and $D_{3/2}$ amplitudes. The lower curve is the $P_{1/2}$ contribution alone.

the $P_{1/2}$ partial cross section and the upper line is the sum of the $P_{1/2}$ and $D_{3/2}$ partial cross sections. It should be noted that for $300 \text{ MeV} < T_\pi < 705 \text{ MeV}$ the $D_{3/2}$ amplitude is dominant in reaction (1) and that the two amplitudes are comparable in reaction (2). Above 750 MeV the $D_{3/2}$ partial cross section would, if a_3 were to

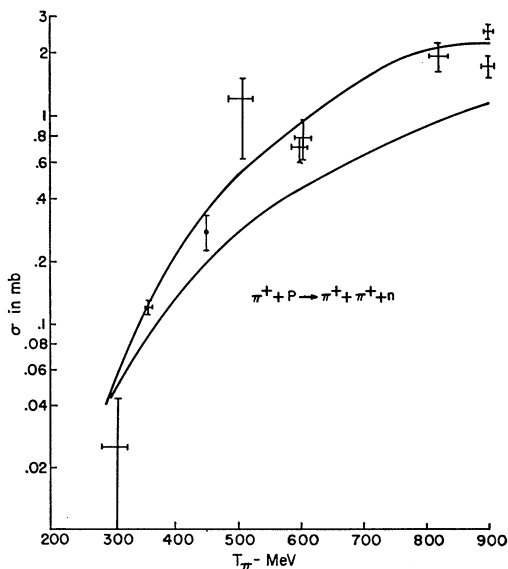


FIG. 9. Cross sections for the reaction $\pi^+ + p \rightarrow \pi^+ + \pi^+ + n$. The upper curve results from using both the $P_{1/2}$ and $D_{3/2}$ amplitudes while the $P_{1/2}$ amplitude alone gives the lower curve.

remain constant, violate inelastic unitarity. Thus, as was discussed in Sec. IV, we decrease a_3 above 750 MeV in such a manner that unitarity is obeyed.

From knowledge of the magnitudes of a_3 and c_3 , the energy distributions may now be predicted. To see what the π - π mass distributions should look like we note from (4.13) and Table I that $\text{Re}(a^*b)$ is negative in reaction (1) and positive in reaction (2). From (5.1) this means that reaction (1) will be enhanced at large π - π masses whereas reaction (2) will be depressed. Figure 10 shows a comparison with experimental $Q(\pi^+\pi^0)$ distributions at $T_\pi=600$ (Ref. 39) and 820 (Ref. 40) MeV (where $Q = M_{\pi\pi} - 2m_\pi$). A similar comparison for the $Q(\pi^+\pi^+)$ distributions in reaction (2) is shown in Fig. 11 for $T_\pi=357$ (Ref. 41) and 600 (Ref.

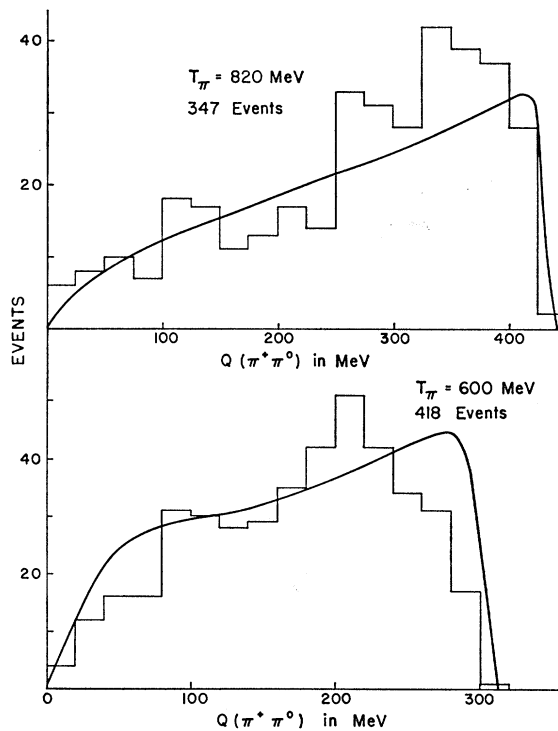


FIG. 10. $\pi^+\pi^0$ mass distributions in the reaction $\pi^+ + p \rightarrow \pi^+ + \pi^0 + p$ at 600 MeV (Ref. 39) and 820 MeV (Ref. 40).

39) MeV. The ratio of reaction (1) to reaction (2) as a function of $Q(\pi\pi)$ is given in Fig. 12 at $T_\pi=820$ MeV.⁴⁰ This last plot is quite sensitive to the angular-momentum properties of the amplitude used. The model developed herein gives a satisfactory description of these distributions.

The angular distributions are primarily determined by (1) the angular-momentum properties of the dominant state and (2) interference between the dominant

³⁹ P. Newcomb, Phys. Rev. **132**, 1283 (1963).

⁴⁰ R. Barloutaud, J. Heughebaert, A. Leveque, C. Louedec, J. Meyer, and D. Tycho, Nuovo Cimento **27**, 238 (1963).

⁴¹ J. Kirz, J. Schwartz, and R. Tripp, Phys. Rev. **126**, 763 (1962); R. Tripp (private communication).

amplitude and the second most important amplitude. If the parities of these two amplitudes are different, odd powers of $\cos\theta$ will be present. By referring to Fig. 8, we see that at intermediate energies the contribution of the $P_{1/2}$ amplitude to reaction (1) is very small, and thus it is quite possible that it is not the second most important amplitude in this reaction. In fact, at 600 (Ref. 39) and 820 (Ref. 40) MeV the angular distributions in reaction (1) are strongly asymmetric and can be explained by the presence of other background terms.² In the case of reaction (2), Fig. 9 shows that the $D_{3/2}$ and $P_{1/2}$ contributions are quite comparable, and thus the angular-distribution predictions should be reliable.

The interference between the $P_{1/2}$ and $D_{3/2}$ amplitudes gives a $\cos\theta$ term whose sign depends upon the

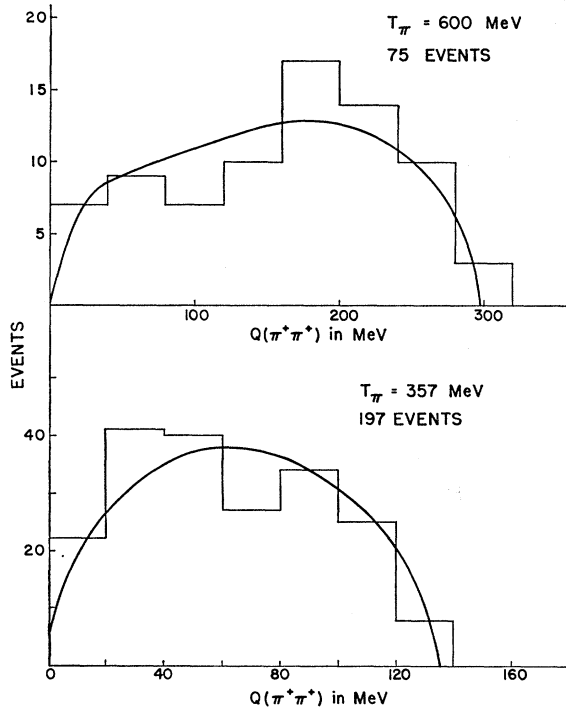


FIG. 11. $\pi^+\pi^+$ mass distributions in the reaction $\pi^+ + p \rightarrow \pi^+ + \pi^+ + n$ at 357 MeV (Ref. 41) and 600 MeV (Ref. 39).

sign of c_3 and also upon χ . At moderate energies (e.g., below 600 MeV) χ should remain small since we are far from the unitary limit and hence the only free parameter is the sign of c_3 . If this sign is chosen to be negative, then the signs of the angular asymmetries are correct for both the π^+ and the neutron in reaction (2). This is shown in Fig. 13 in a comparison with experiment at $T_\pi=357$ (Ref. 41) and 600 MeV (Ref. 39).

To summarize the fit to the π^+p inelastic reactions, we can say that the cross sections, energy distributions, and angular distributions for the $\pi^+\pi^+n$ channel are reasonably described by the two amplitudes $D_{3/2}$ and

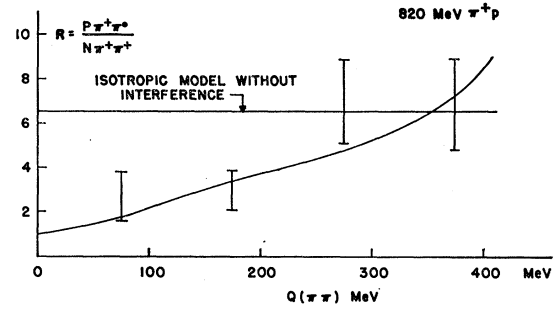


FIG. 12. The ratio $\sigma(\pi^+\pi^0p)/\sigma(\pi^+\pi^+n)$ plotted as a function of $\pi-\pi$ Q value for $T_\pi=820$ MeV (Ref. 40).

$P_{1/2}$ below 800 MeV. Next, we discuss the π^-p reactions and determine the $T=\frac{1}{2}$ amplitudes.

B. π^-p Reactions

When π^-p inelastic reactions are considered,

$$(3) \quad \pi^- + p \rightarrow \pi^- + \pi^0 + p$$

$$(4) \quad \rightarrow \pi^- + \pi^+ + n$$

$$(5) \quad \rightarrow \pi^0 + \pi^0 + n,$$

the effects of both $T=\frac{1}{2}$ and $T=\frac{3}{2}$ amplitudes must be taken into account. Since the $T=\frac{3}{2}$, parameters have already been found, the remaining four parameters to be determined are a_1 , c_1 , Φ , and θ .

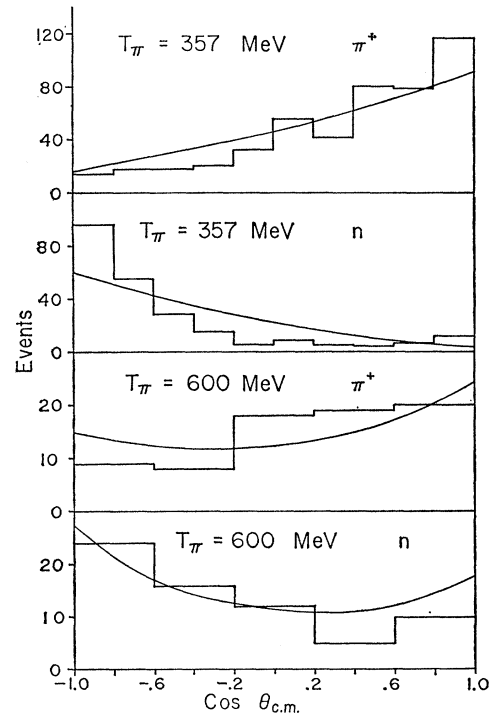


FIG. 13. Angular distributions of the π^+ and neutron in the reaction $\pi^+ + p \rightarrow \pi^+ + \pi^+ + n$ at 357 MeV (Ref. 41) and 600 MeV (Ref. 39). The curves drawn are the model predictions using $P_{1/2}$ and $D_{3/2}$ amplitudes with c_3 negative.

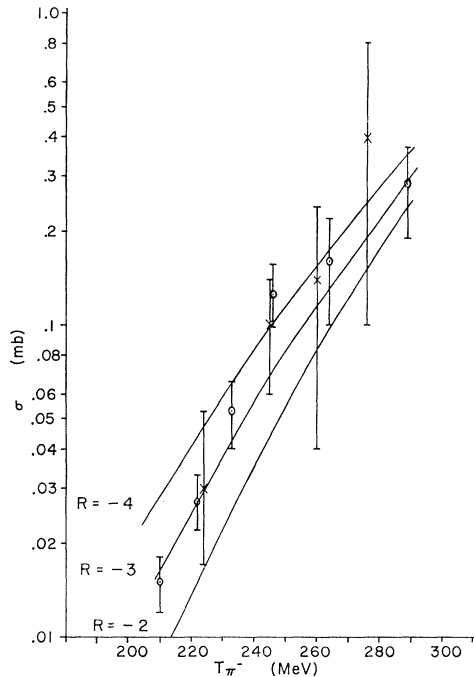


FIG. 14. Threshold behavior of the cross section for the reaction $\pi^- + p \rightarrow \pi^- \pi^+ + n$. The curves are the model predictions for various values of the parameter $R = c_1/c_3$.

As threshold is approached, the $P_{1/2}$ amplitude becomes dominant. Thus the important parameters are c_1 and c_3 (θ being small at threshold). At low energies reaction (4) has been studied most intensively. In Sec. VI we show that there are almost a dozen cross-section measurements below $T_\pi = 300$ MeV. From Table I it follows that the rate for this reaction is proportional to $(2R+1)^2$, where $R = c_1/c_3$. We do not, however, know the sign of R . It will be shown below that, in order to account for angular distributions, R must be negative. Assuming this, we show in Fig. 14 the threshold behavior of reaction (4), the solid lines being the model prediction for different values of R . From this graph we can estimate that

$$\begin{aligned} R &= -2.8 \pm 0.3, \\ c_1 &= 0.285 \pm 0.03 F. \end{aligned} \quad (5.3)$$

From a knowledge of the cross sections for the five production reactions, the pure $T = \frac{1}{2}$ reaction cross section can be calculated using (2.1). Using the compiled experimental data of Sec. VI, $\sigma(T = \frac{1}{2})$ is shown in Fig. 15. The $T = \frac{1}{2}$ cross section can only depend on (in our model) the magnitudes of c_1 and a_1 . Since $|c_1|$ is known, $|a_1|$ can be determined by comparison with the experimental data. The dashed line in Fig. 15 is the model prediction with a constant ratio of $|a_1|/a_3 \approx 4$, which fits the experimental data below 400 MeV. The $D_{3/2}$ ($T = \frac{1}{2}$) amplitude with this ratio is quite large and causes a violation of the inelastic unitarity limit near 400 MeV. If we use our prescription and decrease $|a_1|$ smoothly such that the unitarity maximum is never

exceeded, then the model calculation is given by the solid line in Fig. 15. The actual energy variation imposed in this way on $|a_1|$ is shown in Fig. 16(a). A comparison with data near isobar production threshold gives the following value for $T = \frac{1}{2}$ $D_{3/2}$ amplitude:

$$\begin{aligned} |a_1|/|a_3| &= 3.4 \pm 0.3, \\ a_1 &= 0.059 \pm 0.005 F. \end{aligned}$$

The sign of a_1 will now be determined. From Table I it can be seen that at low energies c_1 makes a negligible contribution to reaction (3).⁴² Since the $T = \frac{1}{2}$ reactions seem to be considerably stronger than the $T = \frac{3}{2}$ reactions, the effects of a_3 will also be negligible. Thus, near isobar production threshold (400 MeV) only the $D_{3/2}$ amplitudes will be important and also the phase Φ should be small. Hence $\sigma(\pi^- p \rightarrow \pi^- \pi^0 p)$ depends only upon a_1 and a_3 . If a_1 is positive, the correct cross section is predicted, but if a_1 is taken to be negative, the cross section is too large by over a factor of 2. Thus we find that sign of a_1 relative to a_3 is positive.

Now we may examine the low-energy angular distributions. Since $P_{1/2}$ contribution is small for $\pi^- \pi^0 p$, the angular distributions in reaction (3) are expected to be quite symmetric according to our model. This is shown to be the case at $T_\pi = 450$ MeV⁴³ in Fig. 17. At $T_\pi = 290$ MeV⁴⁴ the model predictions may be compared

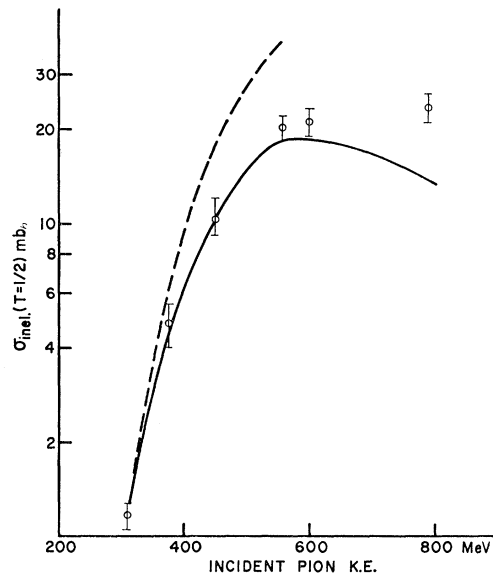


FIG. 15. The $T = \frac{1}{2}$ pion production cross section. The dashed line is calculated with $|a_1|/|a_3| = 4$ independent of energy. The solid line results if this same ratio is used at low energy and the unitarity correction is made.

⁴² In the $\pi\pi$ representation this can be easily seen since the $\pi^- \pi^0$ cannot be in an s -wave state (in the dominant $T = \frac{1}{2}$ reaction) and thus is inhibited for low energies.

⁴³ C. P. Poirier, Ph.D. thesis, Indiana University, 1965 (unpublished), and private communication.

⁴⁴ Yu. A. Batusov, N. Bagachev, S. Bunyatov, V. Sidoriv, and Y. Yarba, Dokl. Akad. Nauk SSSR 133, 52 (1960) [English transl.: Soviet Phys.—Doklady 5, 731 (1961)]; Zh. Eksperim. i Teor. Fiz. 40, 460 (1961) [English transl.: Soviet Phys.—JETP 13, 320 (1961)].

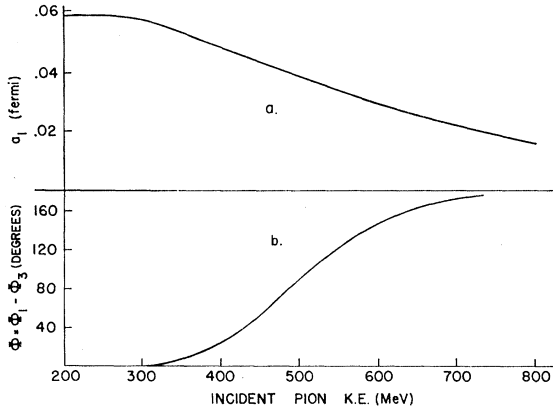


FIG. 16. (a) The energy dependence imposed upon $|a_1|$ by unitarity. (b) The energy dependence required of Φ to simultaneously fit the excitation functions for reactions 4 and 5. The values of Φ at high energy are uncertain since it is clear from Fig. 15 that higher waves become important above 600 MeV.

with experiment in reaction (4). In this case there are strong asymmetries which are adequately reproduced by the model with c_1 positive as shown in Fig. 18. In the absence of experimental data concerning center-of-mass angular distributions for reaction (5), we may predict that the π^0 should be somewhat peaked backward, whereas the neutron should go forward.

The two parameters θ and Φ remain to be determined. Because of the large magnitude of c_1/c_3 and because at higher energies (where θ might be expected to become nonzero) the $P_{1/2}$ amplitude is much smaller than the $D_{3/2}$ amplitude, the available data does not determine θ . On the other hand, the branching ratio into the various charge states is quite sensitive to the magnitude of Φ . From (4.13) and Table I it is seen that at a given energy T_π , increasing $|\Phi|$ increases the cross section for reaction (3) and decreases the cross section for reaction (4). Figure 19 (dashed line) shows the model predictions for these reactions if $|\Phi|$ remains zero. The experimental situation is represented by the solid lines in this same graph. Only if $|\Phi|$ increases sharply in the manner shown in Fig. 16(b) does the model prediction and the experimental points coincide.

Cross sections are sensitive to the magnitude of Φ but not to its sign; however, the sign of Φ can be determined by looking at the Dalitz plot in reaction (3). The asymmetry in the two halves of the Dalitz plot bounded by the line $T_{\pi^0} = T_{\pi^-}$ is quite sensitive to the sign of Φ , and at $T_\pi = 558$ MeV⁴⁵ heavily favors a positive sign.²⁹ Because of the weakness of the $T = \frac{3}{2}$ inelastic reactions relative to the $T = \frac{1}{2}$ reactions in this energy region, we expect $|\Phi_3|$ to be smaller than $|\Phi_1|$, which implies that Φ_1 increases in a positive manner, passing through 90° near $T_\pi = 500$ MeV.

⁴⁵ R. Burnstein, G. Charlton, T. Day, G. Quarenì, A. Quarenì-Vignudelli, G. Yodh, and I. Nadelhaft, Phys. Rev. **137**, B1044 (1965).

As we have seen in (4.7), the phase Φ_1 is closely related to the $D_{3/2}$ elastic phase shift at the same energy, the relationship becoming an equality near threshold. Therefore, our analysis implies that the elastic pion-nucleon amplitude resonates in the $D_{3/2}$ ($T = \frac{1}{2}$) state. Two-body data have shown that the $N_{1/2}^*(1512)$ resonance (which appears in the π^-p elastic cross section) has spin $\frac{3}{2}$ and negative parity.^{6,7} It is thus useful to have an independent verification of the quantum numbers of this resonance.

All the parameters of the $D_{3/2}$ and $P_{1/2}$ amplitudes have been determined. Using these parameters, we compare model results with the experimental compilations of cross sections for reaction (3) in Fig. 20, for reaction (4) in Fig. 21, and for reaction (5) in Fig. 22. The accurate prediction of the cross section in reaction (5) is significant since we have not used this data at all in the parameter determination. As in the π^+p case, the lower curves in Figs. 20, 21, and 22 are the $P_{1/2}$ partial cross section, and the upper curves are the sum of the $P_{1/2}$ and $D_{3/2}$ contributions.

Finally, we discuss the energy distributions. Figure 23 shows these distributions in the case of reaction (3) at $T_\pi = 558$ MeV.⁴⁵ It is seen that the model predicts an enhancement for large $Q(\pi^-\pi^0)$ values which agrees with the experimental distribution. At the same energy Fig. 24 shows the corresponding energy distributions for reaction (4). In this case no enhancement is expected at high $\pi^-\pi^+$ masses in our model. As is seen,

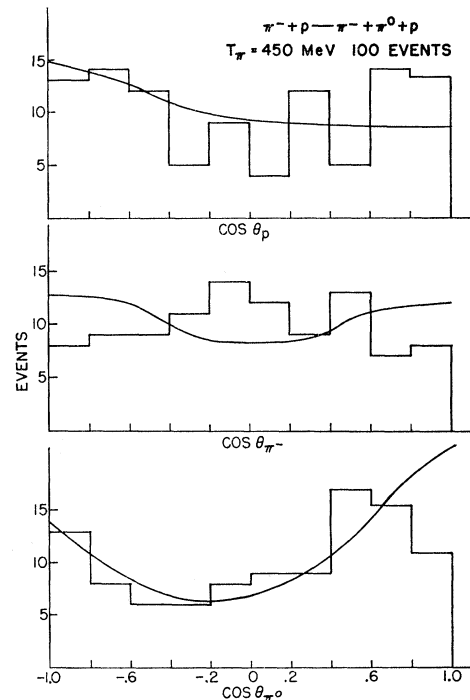


FIG. 17. Angular distributions in the over-all c.m. for the reaction $\pi^- + p \rightarrow \pi^- + \pi^0 + p$ at 450 MeV (Ref. 43). The curves are calculated with both the $P_{1/2}$ and $D_{3/2}$ amplitudes.

the experimental data contradict this prediction. This discrepancy occurs over a wide range of incident energies being particularly evident near $T_\pi = 400$ MeV.⁴⁶ A similar effect seems to occur in reaction (5), although the experimental data for this reaction is rather meager.⁴⁷ The existence of substantial deviations in the $\pi\pi$ mass spectra for reactions (4) and (5) strongly suggests that the $T=0$ $\pi\pi$ state has some strong final-state interaction.²²

When this "anomalous" effect is most evident, the $\pi\pi$ mass peaking occurs at about 400 MeV, which suggests that this peak results from the decay of the proposed σ meson.⁴⁸ However, it is difficult to explain the observed peaking⁴⁶ of the $\pi\pi$ mass at the upper end as T_π increases and the kinematic limit of the $\pi\pi$ mass exceeds 400 MeV. Recently, a model of this sort has been proposed by Thurnauer⁴⁹ which requires the σ mass to be 490 MeV to account for the observed distributions.

Another possible mechanism to account for the observed peaking would be to produce an ABC enhancement.⁵⁰ This amplitude could be made to interfere

destructively with the s -wave $N^*(3,3)$ amplitude or equivalently with the $P_{1/2}^+$ amplitude considered herein which could enhance large $\pi\pi$ masses over a wide range of T_π .

Another approach has been suggested by Anisovich and Dakhno.⁴ They have shown that if the pion from the decaying $N^*(3,3)$ rescatters with the "extra" pion (a triangle diagram), it is possible to account for the anomalous peaking in a quite satisfactory manner. However, the model used by these authors was oversimplified in that angular-momentum barriers were neglected and the nonrescattered part (s -wave N^* production) was represented by an undetermined constant. Both these faults would in principle be circumvented by a more detailed calculation of the triangle diagram and by using the N^* production amplitude determined by the method of this paper. This being so, the only free parameter is the $\pi\pi$ scattering length. A further discussion of this is contained in another paper.⁵¹ Of course, it is possible that more than one mechanism (σ , ABC, triangle diagrams) may be contributing simultaneously to give rise to the "anomalous"

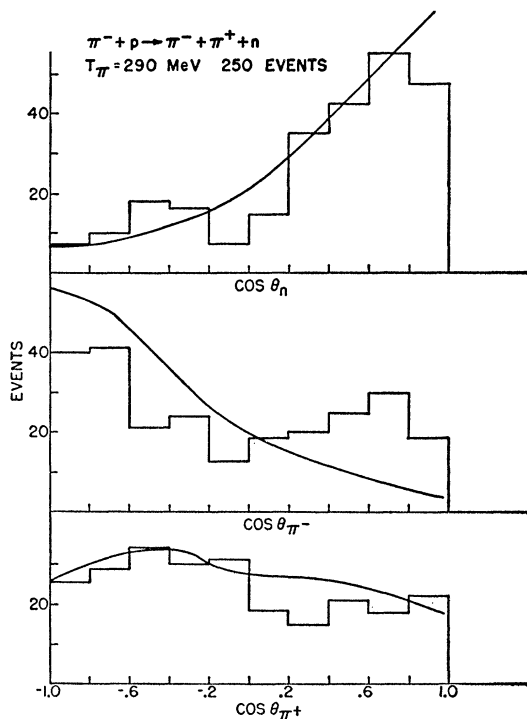


FIG. 18. Angular distributions in the over-all c.m. for the reaction $\pi^- + p \rightarrow \pi^- + \pi^+ + n$ at 290 MeV (Ref. 44). The curves are calculated with both the $P_{1/2}$ and $D_{3/2}$ amplitudes and with c_1 positive.

⁴⁶ J. Kirz, J. Schwartz, and R. Tripp, Phys. Rev. **130**, 2481 (1963).

⁴⁷ B. Barish, R. Kurz, V. Perez-Mendez, and J. Solomon, Phys. Rev. **135**, B416 (1964).

⁴⁸ L. Brown and P. Singer, Phys. Rev. **133**, B812 (1964).

⁴⁹ P. Thurnauer, Phys. Rev. Letters **14**, 985 (1965).

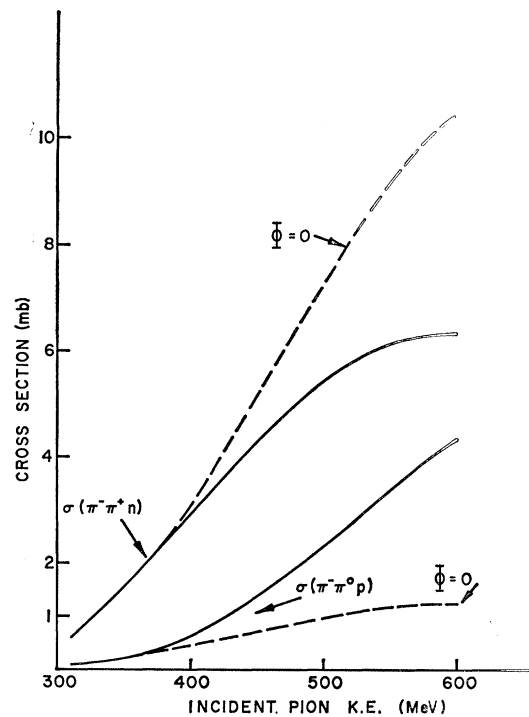


FIG. 19. The dependence of the excitation functions of the reactions $\pi^- + p \rightarrow \pi^- + \pi^+ + n$ and $\pi^- + p \rightarrow \pi^- + \pi^0 + p$ upon the parameter Φ [the interference angle between $T=\frac{1}{2}$ and $T=\frac{3}{2}$ $N^*(3,3)$ production]. The dashed curve results if Φ remains zero. If Φ increases in the manner of Fig. 16(b) the solid curve is generated. This later curve is a good fit to the experimental data.

⁵⁰ N. Booth, A. Abashian, and K. Crowe, Phys. Rev. **122**, 2309 (1964).

⁵¹ C. Kacsar, M. Olsson, and G. Yodh, in *Proceedings of the Oxford International Conference on Elementary Particles, 1965* (Rutherford High Energy Laboratory, Harwell, England, 1966).

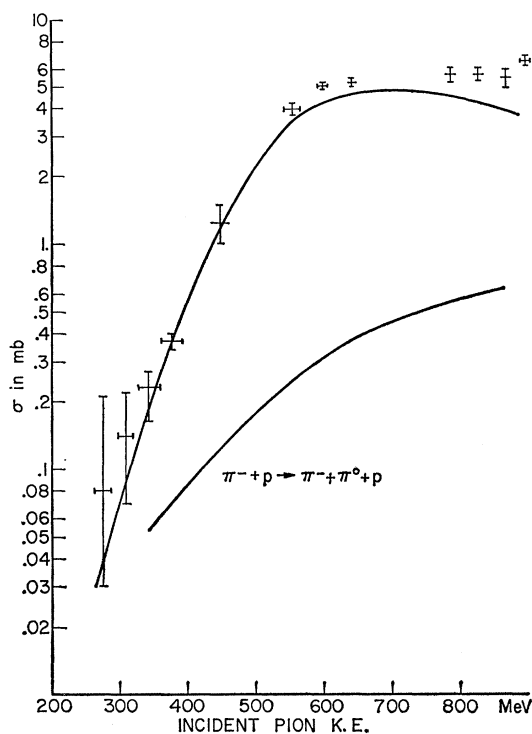


FIG. 20. Cross sections for the reaction $\pi^- + p \rightarrow \pi^- + \pi^0 + p$. The upper curve results from using both the $P_{1/2}$ and $D_{3/2}$ amplitudes while the $P_{1/2}$ amplitude alone gives the lower curve.

peaking. It seems to be very difficult to get a unique solution to this problem.

VI. DATA COMPILATION

This section contains a collection of all the experimental references known to the authors for the five single-pion production reactions in the energy range studied.^{52,50-71} To increase the usefulness of this com-

⁵² V. Barnes, D. Bugg, I. Derado, A. Minguzzi, L. Montanet, R. Van De Walle, R. Carrara, M. Cresti, A. Grigoletto, A. Loria, L. Peruzzo, and R. Santangelo, CERN Report 63-27 (unpublished).

⁵³ References to several analyses of this type are found in P. Bareyre *et al.* (Ref. 7).

⁵⁴ W. Willis, *Phys. Rev.* **116**, 753 (1959).

⁵⁵ J. Detoeuf, Y. Ducros, J. Merlo, A. Stirling, B. Thevenet, L. Van Rossum, and J. Zsembery, *Phys. Rev.* **134**, B228 (1964).

⁵⁶ R. Barloutaud, L. Cardin, A. Derem, C. Gensollen, A. Leveque, C. Louedec, J. Meyer, and D. Tycho, *Nuovo Cimento* **26**, 1409 (1962).

⁵⁷ C. A. Tilger, C. P. Poirier, E. D. Alyea, H. J. Martin, Jr., and J. H. Scandrett, *Phys. Rev.* **142**, 972 (1966).

⁵⁸ C. Gensollen, P. Granet, R. Barloutaud, A. Leveque, and J. Meyer, in *Proceedings of the Sienna International Conference on Elementary Particles and High Energy Physics, 1963*, edited by G. Bernardini and G. P. Puppi (Società Italiana di Fisica, Bologna, 1963), Vol. 1, p. 84.

⁵⁹ D. Stonehill, Ph.D. thesis, Yale University, 1962 (unpublished); earlier results are given in D. Stonehill, C. Baltay, H. Courant, W. Fickinger, E. Fowler, H. Kraybill, J. Sandweiss, J. Sanford, and H. Taft, *Phys. Rev. Letters* **6**, 624 (1961).

⁶⁰ Yu. Batusov, S. Bunyatov, V. Sidorov, and V. Jarba, *JINR-P-1823* and *JINR-P-1838* (unpublished).

⁶¹ J. Deahl, M. Derrick, J. Fetkovich, T. Fields, and G. Yodh, *Phys. Rev.* **124**, 1987 (1961).

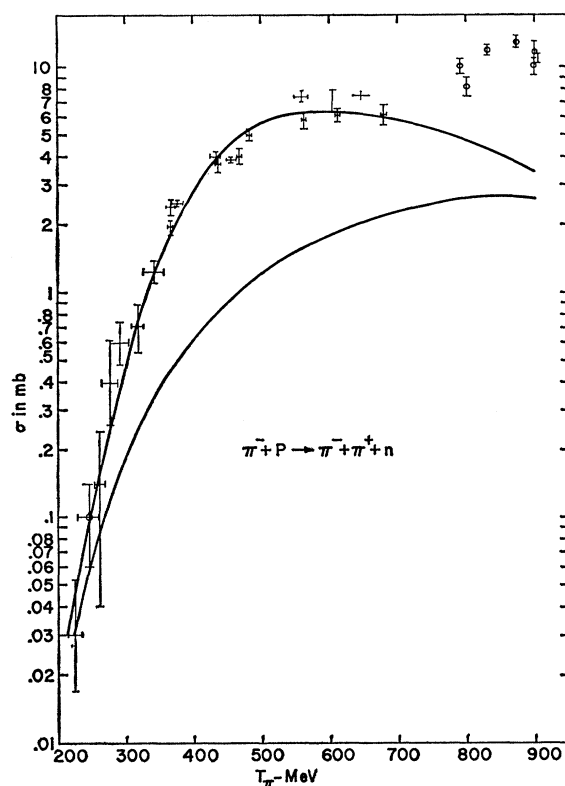


FIG. 21. Cross sections for the reaction $\pi^- + p \rightarrow \pi^- + \pi^+ + n$. The upper curve is calculated using the $P_{1/2}$ and $D_{3/2}$ amplitudes. The lower curve is the $P_{1/2}$ contribution alone.

pilation we list the kinetic energy and cross section for each experiment. Only experiments which directly measure the production process are considered. The

⁶² Yu. Batusov, S. Bunyatov, V. Sidorov, and V. Jarba, *Zh. Eksperim. i Teor. Fiz.* **39**, 1850 (1960) [English transl.: *Soviet Phys.—JETP* **12**, 1290 (1961)].

⁶³ W. Perkins, J. Caris, R. Kenney, and V. Perez-Mendez, *Phys. Rev.* **118**, 1364 (1960).

⁶⁴ T. Blokhintseva, V. Grebinnik, V. Zhukov, G. Libman, L. Nemenov, G. Selivanov, and Y. Jung-Fang, *Zh. Eksperim. i Teor. Fiz.* **44**, 498 (1963) [English transl.: *Soviet Phys.—JETP* **17**, 340 (1963)].

⁶⁵ T. Blokhintseva, V. Grebinnik, V. Zhukov, G. Libman, L. Nemenov, G. Selivanov, and Y. Jung-Fang, in *Proceedings of the Twelfth Annual International Conference on High Energy Physics, Dubna, 1964* (Atomizdat, Moscow, 1965). Earlier results of these authors are found in *Zh. Eksperim. i Teor. Fiz.* **42**, 912 (1962); **44**, 116 (1963) [English transl.: *Soviet Phys.—JETP* **15**, 629 (1962); **17**, 80 (1963)].

⁶⁶ J. Brisson, P. Falk-Vairant, J. Merlo, P. Sonderegger, R. Turlay, and G. Valladas, *The Aix-en-Provence International Conference on Elementary Particles, 1961*, edited by E. Cremieu-Alcon *et al.* (Centre d'Etudes Nucleaires de Saclay, Seine-et-Oise, France, 1961), Vol. 1, p. 45; R. Turlay, thesis, Rapport CEA-2136 (unpublished).

⁶⁷ C. Vittitoe, B. Riley, W. Fickinger, V. Kenney, J. Mowat, and W. Shephard, *Phys. Rev.* **135**, B232 (1964).

⁶⁸ J. Oliver, I. Nadelhaft, J. Ashkin, and G. Yodh, *Bull. Am. Phys. Soc.* **9**, 80 (1964); J. Oliver, Ph.D. thesis, Carnegie Institute of Technology, 1965 (unpublished).

⁶⁹ V. Kenney, J. Stautberg, and C. Vittitoe, *Bull. Am. Phys. Soc.* **8**, 523 (1963); and private communication.

⁷⁰ E. Pickup, D. Robinson, E. Salant, F. Ayer, and B. Munir, *Phys. Rev.* **132**, 1819 (1963).

⁷¹ J. Massimo, Ph.D. thesis, Brown University, 1964 (unpublished).

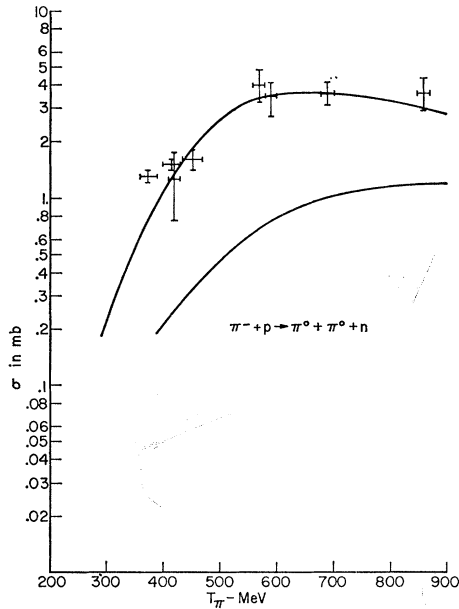


FIG. 22. Cross sections for the reaction $\pi^- + p \rightarrow \pi^0 + \pi^0 + n$. The meaning of the curves is the same as in Figs. 20 and 21. This reaction was not used in determining the parameters and thus checks consistency of the model.

method of subtraction from the total cross section gives only a limited amount of information and would seem to be more susceptible to error.⁵³ The compiled cross sections are contained in Tables II and III.

VII. CONCLUSIONS

A simple model has been constructed to make a phenomenological investigation of the single-pion-production process at low energies. An amplitude for s -wave production of the $N^*(3,3)$ resonance has been used in conjunction with a threshold amplitude in which all of the particles are in s waves. It is found that this model

TABLE II. Compilation of experiments measuring the cross sections for reactions $\pi^+ + p \rightarrow \pi^+ + \pi^0 + p$ and $\pi^+ + p \rightarrow \pi^+ + \pi^+ + n$. (The cross sections are all measured in millibarns.)

T_π (MeV)	($+0p$)	($++n$)	Reference
300	0.11 ± 0.04	0.025 ± 0.018	52
357		0.12 ± 0.01	41
450	1.04 ± 0.2	0.29 ± 0.06	43
500	1.7 ± 0.8	1.1 ± 0.3	54
	-0.3	-0.7	
520	1.3 ± 0.5		55
600	3.8 ± 0.3	0.7 ± 0.1	39
600	3.55 ± 0.53	0.78 ± 0.17	56
615	3.6 ± 0.5		55
660	5.5 ± 0.5		55
710	7.8 ± 0.5		55
760	9.7 ± 0.5		55
780	12.2 ± 1.4	2.8 ± 0.4	57
815	10.1 ± 0.5		55
820	9.3 ± 0.8	1.9 ± 0.3	40
900	7.5 ± 0.5	1.7 ± 0.2	58
900	8.6 ± 0.8	2.4 ± 0.4	40
910	10.5 ± 0.4	2.5 ± 0.2	59

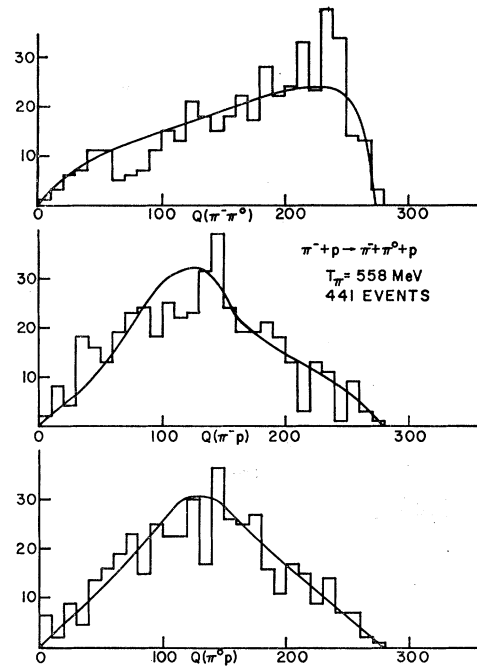


FIG. 23. Q -value distributions for the reaction $\pi^- + p \rightarrow \pi^- + \pi^0 + p$ at 558 MeV (Ref. 45). Adequate fits are obtained over a wide range of energies for this reaction.

is able to account for most of the experimental phenomena in a natural way, by which we mean that the parameters determined by comparison with the experimental data are found to be constants or to vary in a

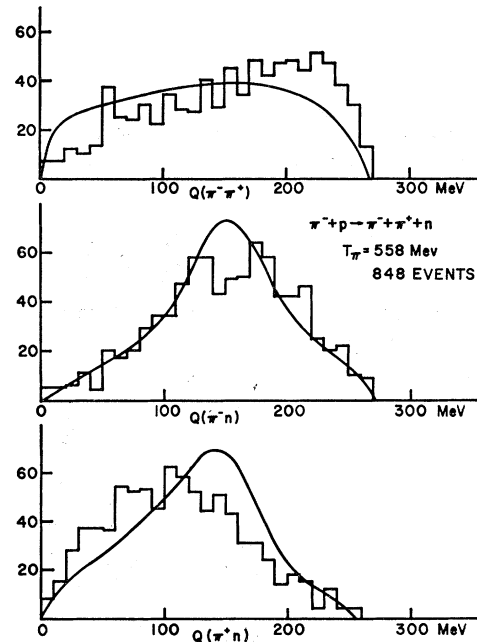


FIG. 24. Q -value distributions for the reaction $\pi^- + p \rightarrow \pi^- + \pi^+ + n$ at 558 MeV (Ref. 45). This figure illustrates the "anomalous" $\pi\pi$ peaking effect. The π^-n projection still fits since it is dominated by N^* production.

TABLE III. Compilation of experiments measuring the cross sections. For reactions $\pi^+p \rightarrow \pi^+\pi^0+p$, $\pi^-p \rightarrow \pi^-\pi^0+p$, $\pi^-p \rightarrow \pi^-\pi^+\pi^0+n$, and $\pi^-p \rightarrow \pi^0+\pi^0+n$. (The cross sections are all measured in millibarns.)

T_π (MeV)	($-0p$)	($-+n$)	($00n$)	Refer- ence
210		0.015±0.003		60
222		0.027±0.005		60
224		0.03 ±0.02		61
233		0.053±0.013		60
245		0.10 ±0.04		62
246		0.125±0.028		60
260		0.14 ±0.10		63
264		0.16 ±0.06		60
276	0.08+0.13 -0.05	0.4 +0.2 -0.3		64
288		0.28 ±0.09		60
290		0.61 ±0.13		44
310	0.13±0.06			47
317		0.71 ±0.17		63
344	0.23+0.04 -0.07	1.5 ±0.1		65
365		2.4 ±0.2		47
365		1.93 ±0.16		46
371		1.93 ±0.37		63
374		2.6 ±0.2	1.3 ±0.1	47
377	0.31+0.07 -0.04			47
417		3.3 ±0.3	1.5 ±0.1	47
421			1.25±0.5	66
427		3.36 ±0.74		63
432		4.0 ±0.2		47
435		3.7 ±0.3		46
450	1.58±0.2	5.2 ±0.64		43
454		3.8 ±0.4	1.6 ±0.2	47
466		4.0 ±0.3		46
470			0.85±0.75	66
480		5.0 ±0.3		46
558	4.0 ±0.5	7.5 ±0.8		45
570			4.1 ±0.8	66
590			3.4 ±0.7	66
604	4.98±0.54	7.87 ±0.91		67
646	4.65±0.17	7.14 ±0.23		68
690			3.6 ±0.5	66
790	5.62±0.52	10.0 ±0.78		69
800	3.9 ±0.5	8.2 ±0.8		58
830	5.69±0.52	11.95 ±0.87		69
865			3.6 ±0.7	66
870	5.39±0.54	12.88 ±0.99		69
900	5.7 ±0.6	10.1 ±0.9		58
905	6.5 ±0.5	10.7 ±0.6		70
905	5.0 ±0.7			71

simple manner. The model provides a systematic method for investigating the properties of the production process, many of which are not easily apparent in the raw data. The main conclusions are:

1. The rapid variation of the ratio $\sigma(\pi^+p \rightarrow \pi^+\pi^0p)/\sigma(\pi^+p \rightarrow \pi^+\pi^+n)$ as shown in Fig. 3 is explained as an angular-momentum barrier effect inhibiting the isobar production process as threshold is approached.

2. The peaking at large $\pi^+\pi^0$ mass in the reaction $\pi^+p \rightarrow \pi^+\pi^0+p$, which had once been considered as evidence for the ζ meson,⁴⁰ is found to be an effect caused by interference between the two charge states of s -wave isobar production.

3. Above 600 MeV in the reaction $\pi^+p \rightarrow \pi^+\pi^0+p$ there is evidence from the angular distribution that higher wave isobar production is becoming important.

4. From the growth rates of the reactions $\pi^-+p \rightarrow \pi^-+\pi^0+p$ and $\pi^-+p \rightarrow \pi^-+\pi^++n$ it can be inferred that the phase of the $T=\frac{1}{2}$ isobar production process increases rapidly, and hence by unitarity, it may be concluded that the $D_{3/2}$ elastic amplitude resonates near $T_\pi=600$ MeV.

5. The peaking in the $\pi^+\pi^-$ mass shown by Kirz *et al.*⁹ is established as anomalous behavior not explained by this simple model.²²

6. The magnitudes and signs of the amplitudes for threshold production and s -wave isobar production have been determined from the experimental data.

7. It is apparent that above $T_\pi=600$ MeV, higher partial waves must enter in an important way to account for the $T=\frac{1}{2}$ cross section (e.g., Fig. 15).

Finally, it should be remarked that our model uses an isobar production parameter which is constant in magnitude (except for a smooth variation imposed by unitarity). It is found that the π^-p reaction cross sections are satisfactorily accounted for in the region of the first $T=\frac{1}{2}$ resonance ($T_\pi=600$ MeV). Recent data,^{45,67,68} however, show a slight bump of about 10% at 600 MeV. Aside from this, all the evidence of resonant behavior in the inelastic $D_{3/2}$ state comes from the rapid variation of the production phase.

APPENDIX A

To derive the angular distribution formula (4.5) from (4.4)

$$J(\mu_1) = 4\pi \int_0^\pi |M|^2 d\eta_1, \quad (4.4)$$

$$\mu_2 = \mu_0\mu_1 + \sin\theta_0 \sin\theta_1 \cos\eta_1,$$

expand $|M|^2$ as follows:

$$|M|^2 = \sum_{l,n} a_{ln} P_l(\mu_1) P_n(\mu_2),$$

and use the usual Legendre-polynomial addition formula

$$P_n(\mu_2) = P_n(\mu_0)P_n(\mu_1) + 2 \sum_{m=1}^n ((n-m)!/(n+m)!) \times P_n^m(\mu_0)P_n^m(\mu_1) \cos m\eta_1.$$

Now the integrals may be performed leaving

$$J(\mu_1) = 4\pi^2 \sum_{l,n} a_{l,n} P_n(\mu) P_l(\mu_1) P_n(\mu_1); \quad (A1)$$

the desired form

$$J(\mu_1) = 2\pi^2 \sum_{l=0}^{\infty} (2l+1) \int_{-1}^{+1} d\mu_2 |M|^2 \times P_l(\mu_0) P_l(\mu_1) P_l(\mu_2) \quad (4.5)$$

is now easily shown to be equivalent to (4.4) by using the same expansion of $|M|^2$ and comparing terms with (A1).

**APPENDIX B: LORENTZ TRANSFORMATION
FROM THE OVER-ALL CENTER OF
MOMENTUM TO THE REST
SYSTEM OF TWO OF
THE PARTICLES**

We want to transform from the over-all rest system in which

$$\mathbf{P}_1 + \mathbf{P}_2 + \mathbf{P}_3 = 0$$

to one in which the momenta \mathbf{P}_2' and \mathbf{P}_3' add to zero and the other particle has momentum π_1 (and energy ϵ_1). To accomplish this we need a pure Lorentz transformation parallel to \mathbf{P}_1

$$\pi_1 = \gamma_1(P_1 - \beta_1 E_1), \quad \epsilon_1 = \gamma_1(E_1 - \beta_1 P_1).$$

Consider the Lorentz scalar $L_0 = (q_1 + q_2 + q_3)$ where q_i are momentum 4 vectors. In the three-particle rest frame $L_0 = E_0^2$ is the total energy squared. L_0 evaluated in the two-particle rest frame is $(\epsilon_1 + \omega_{23})^2 - \pi_1^2$, where $\omega_{23} = E_2' + E_3'$,

$$\omega_{23}^2 = (q_2 + q_3)^2 = (E_2' + E_3')^2 = E_0^2 + m^2 - 2E_0 E_1.$$

This relation leads to

$$\epsilon_1 = (E_0 E_1 - m^2) / \omega_{23}, \quad \pi_1 = (E_0 / \omega_{23}) P_1,$$

giving directly

$$\beta_1 = -P_1 / (E_0 - E_1), \quad \gamma_1 = (E_0 - E_1) / \omega_{23}.$$

Thus, in order to express quantities in the two-particle

rest system in terms of over-all rest-system quantities, we use a Lorentz transformation velocity

$$\mathbf{V} = -\mathbf{P}_1 / (E_0 - E_1).$$

The correct transformations are well known⁷² to be

$$\mathbf{P}_2' = \mathbf{P}_2 + \mathbf{V}[(\mathbf{V} \cdot \mathbf{P}_2 / \beta_1^2)(\gamma_1 - 1) - \gamma_1 E_2],$$

$$E_2' = \gamma(E_2 - \mathbf{V} \cdot \mathbf{P}_2)$$

leading to

$$\mathbf{P}_2' = \mathbf{P}_2 + (\mathbf{P}_1 / \omega_{23}) [((E_0 - E_1 - \omega_{23}) / P_1^2) \mathbf{P}_1 \cdot \mathbf{P}_2 + E_2].$$

Note that

$$P_1^2 = (E_0 - E_1 - \omega_{23})(E_0 - E_1 + \omega_{23}),$$

so

$$\mathbf{P}_2' = \mathbf{P}_2 + (\mathbf{P}_1 / \omega_{23}) [(\mathbf{P}_1 \cdot \mathbf{P}_2 / (E_0 - E_1 + \omega_{23})) + E_2],$$

$$E_2' = \omega_{23}^{-1} [(E_0 - E_1) E_2 + \mathbf{P}_1 \cdot \mathbf{P}_2].$$

Or, when these are combined,

$$\mathbf{P}_2' = \mathbf{P}_2 + \mathbf{P}_1 [(E_2 + E_2') / (E_0 - E_1 + \omega_{23})]$$

and similarly for the other isobar rest frame:

$$\mathbf{P}_1' = \mathbf{P}_1 + \mathbf{P}_2 [(E_1 + E_1') / (E_0 - E_2 + \omega_{13})],$$

define

$$X_2 = \frac{E_2 + E_2'}{E_0 - E_1 + \omega_{23}}, \quad X_1 = \frac{E_1 + E_1'}{E_0 - E_2 + \omega_{13}}.$$

⁷² See, for example, C. Møller, *The Theory of Relativity* (Oxford University Press, Oxford, England, 1957), p. 72.